J. Fluid Mech. (2014), *vol.* 739, *pp.* 392–420.
doi:10.1017/jfm.2013.620

A generalized Reynolds analogy for compressible wall-bounded turbulent flows

You-Sheng Zhang[1,2], Wei-Tao Bi[1,†], Fazle Hussain[3] and Zhen-Su She[1]

[1]State Key Laboratory for Turbulence and Complex Systems and Department of Mechanics and Engineering Science, College of Engineering, Peking University, Beijing 100871, China

[2]Institute of Applied Physics and Computational Mathematics, Beijing 100094, China

[3]Department of Mechanical Engineering,Texas Tech University, Lubbock, TX 79409-1021, USA

(Received 7 April 2013; revised 7 October 2013; accepted 17 November 2013;
first published online 20 December 2013)

A generalized Reynolds analogy (GRA) is proposed for compressible wall-bounded turbulent flows (CWTFs) and validated by direct numerical simulations. By introducing a general recovery factor, a similarity between the Reynolds-averaged momentum and energy equations is established for the canonical CWTFs (i.e. pipes, channels, and flat-plate boundary layers that meet the quasi-one-dimensional flow approximation), independent of Prandtl number, wall temperature, Mach number, Reynolds number, and pressure gradient. This similarity and the relationships between temperature and velocity fields constitute the GRA. The GRA relationship between the mean temperature and the mean velocity takes the same quadratic form as Walz's equation, with the adiabatic recovery factor replaced by the general recovery factor, and extends the validity of the latter to diabatic compressible turbulent boundary layers and channel/pipe flows. It also derives Duan & Martín's (*J. Fluid Mech.*, vol. 684, 2011, pp. 25–59) empirical relation for flows at different physical conditions (wall temperature, Mach number, enthalpy condition, surface catalysis, etc.). Several key parameters besides the general recovery factor emerge in the GRA. An effective turbulent Prandtl number is shown to be the reason for the parabolic profile of mean temperature versus mean velocity, and it approximates unity in the fully turbulent region. A dimensionless wall temperature, that we call the diabatic parameter, characterizes the wall-temperature effects in diabatic flows. The GRA also extends the analysis to the fluctuation fields. It recovers the modified strong Reynolds analogy proposed by Huang, Coleman & Bradshaw (*J. Fluid Mech.*, vol. 305, 1995, pp. 185–218) and explains the variation of the temperature–velocity correlation coefficient with wall temperature. Thus, the GRA unveils a generalized similarity principle behind the complex nonlinear coupling between the thermal and velocity fields of CWTFs.

Key words: compressible boundary layers, compressible turbulence, turbulence theory

1. Introduction

Compressible wall-bounded turbulent flows (CWTFs) are ubiquitous on the surfaces of high-speed flying vehicles, gas turbine blades, rocket motor nozzles, etc. In these flows, heat transfer is as important as the aerodynamic force (Smits & Dussauge

† Email address for correspondence: weitaobi@pku.edu.cn

2006). For the structure to be safe, efficient, reliable and economical, an accurate estimation of the velocity and thermal fields is needed, which is difficult due to the nonlinear coupling between the kinetic and thermal quantities, affected by varied flow conditions in aerospace applications. The topic has a long history of study, focusing on establishing quantitative relationships between temperature and velocity through the similarity of momentum and energy transport in wall-bounded turbulent flows (Reynolds 1874; Morkovin 1962; Walz 1966; Cebeci & Smith 1974; Gaviglio 1987; Huang, Coleman & Bradshaw 1995; Brun *et al.* 2008). These theories, generally referred to as the Reynolds analogy, have been utilized to develop integral methods to calculate the wall heat flux and the skin friction (Van Driest 1951; Spalding & Chi 1964; Sheshagir & Paranjpe 1969; Hopkins & Inouye 1971; Stalker 2005); they have also been used to develop models for compressible turbulence (Rubesin 1990; Jiang & Campbell 2008).

Being one of the very few theoretical concepts in compressible turbulence, the Reynolds analogy theory continues to attract much attention (Guarini *et al.* 2000; Maeder, Adams & Kleiser 2001; Pirozzoli, Grasso & Gatski 2004; Brun *et al.* 2008; Duan 2011; Pirozzoli & Bernardini 2011). On one hand, these theories are still inadequate in depicting complex flows, e.g. CWTFs with pressure gradient and surface heat flux, for which the mechanism is generally unclear. On the other hand, quantitatively accurate mean-field theories of wall-bounded turbulent flows are now promising, particularly with the help of direct numerical simulation (DNS) data (She *et al.* 2010, 2011 (unpublished observations), 2012), in which the Reynolds analogy theories present a way to decouple the effects of the thermal and velocity fields. With quantitative comparison to DNS data, the Reynolds analogy itself may also be improved and the mechanism elucidated. This is the aim of the present study.

The first temperature–velocity relationship was presented by Reynolds (1874) for incompressible flows through the similarity between the Reynolds-averaged momentum and energy equations – the so-called Reynolds analogy. This theory was then extended to compressible flows. Busemann (1931) and Crocco (1932) independently obtained a relation for compressible laminar boundary layers by assuming unity Prandtl number (Pr, for air $Pr \approx 0.7$). Their derivations were extended to turbulent boundary layers by Van Driest (1951). These studies show that the mean temperature is a quadratic function of the mean velocity:

$$\frac{\bar{T}}{\bar{T}_\delta} = \frac{\bar{T}_w}{\bar{T}_\delta} + \frac{\bar{T}_{c\delta} - \bar{T}_w}{\bar{T}_\delta}\frac{\bar{u}}{\bar{u}_\delta} + \frac{\bar{T}_\delta - \bar{T}_{c\delta}}{\bar{T}_\delta}\left(\frac{\bar{u}}{\bar{u}_\delta}\right)^2, \quad \bar{T}_{c\delta} = \bar{T}_\delta + c\frac{\bar{u}_\delta^2}{2C_p}, \tag{1.1}$$

where T is temperature, u is streamwise velocity, C_p is specific heat at constant pressure, an overbar denotes a Reynolds average, subscript w denotes wall, and subscript δ denotes boundary layer edge ($\delta = \delta_{99}$). The c in (1.1) is a parameter that equals one in the Crocco–Busemann relation, but modified to the recovery factor r of $\sim$0.9 by Walz (1966) to account for the deviation of Pr from unity. Equation (1.1) with $c = r$ was called the modified Crocco–Busemann relation or Walz's equation. Various theories (Whitfield & High 1977), measurements (Laderman & Demetriades 1974; Owen, Horstman & Kussoy 1975; Laderman 1978) and DNS (Gatski & Erlebacher 2002; Pirozzoli *et al.* 2004; Duan 2011) show that Walz's equation improves the Crocco–Busemann relation and agrees with DNS very well in adiabatic compressible turbulent boundary layers (CTBLs). In diabatic CTBLs, however, Walz's equation clearly deviates from DNS (Duan 2011).

Here, we introduce a general recovery factor r_g that includes the effects of Pr, wall temperature, pressure gradient, etc., and derive (1.1) with $c = r_g$. Development of the new relation is based on a generalized similarity between the Reynolds-averaged momentum and energy equations of the CWTFs that meet the quasi-one-dimensional flow approximation. We call this newly derived similarity a generalized Reynolds analogy (GRA). In this paper, the mean relation of the GRA (i.e. (1.1) with $c = r_g$) is validated by DNS of CTBLs, compressible channel flows (CCFs) and compressible pipe flows (CPFs). Duan & Martín (2011) recently presented an empirical relation based on DNS of a broad category of CTBLs. As will be demonstrated, Duan and Martín's relation can be derived by the GRA relation, and their empirical constant is revealed to be the product of Pr and the Reynolds analogy factor s.

Regarding the fluctuation fields, sets of relations with respect to the correlations of the streamwise velocity fluctuation u' and the temperature fluctuation T' have also been proposed. The first set was identified by Morkovin (1962) and known collectively as the strong Reynolds analogy (SRA). The SRA was derived for zero-pressure-gradient adiabatic CTBLs under two assumptions: (*a*) $Pr = 1$; and (*b*) $T_t' = 0$, where $T_t = T + u_i u_i/(2C_p)$ is total temperature. In numerous studies (Gaviglio 1987; Guarini *et al.* 2000; Maeder *et al.* 2001; Duan 2011), most SRA relations have been found invalid. This invalidity was generally ascribed to failure to satisfy assumption (*b*). Later, Cebeci & Smith (1974) extended the SRA to consider the wall heat flux, but the extended SRA is still inadequate in describing the experimental (Gaviglio 1987) and DNS (Duan 2011) data for diabatic flows.

Some modified SRAs, invoking different assumptions, have a common form:

$$\frac{\sqrt{\overline{T'^2}}/\bar{T}}{(\gamma-1)\,M^2\sqrt{\overline{u'^2}}/\bar{u}} = \frac{1}{a\left(1-\partial\bar{T}_t/\partial\bar{T}\right)}, \tag{1.2}$$

where a is chosen to be 1, 1.34, Pr_t (i.e. turbulent Prandtl number) or $1/Pr_m$ (i.e. mixed Prandtl number) in the models proposed by Gaviglio (1987), Rubesin (1990), Huang *et al.* (1995) and Brun *et al.* (2008) respectively, $\gamma = 1.4$ is the ratio of specific heats, $M = \bar{u}/\sqrt{\gamma R\bar{T}}$ is local Mach number, and R is the constant of ideal gas. Among the four modified SRAs, Huang's model (HSRA) agrees best with DNS under different wall temperature conditions and flow situations including external (Guarini *et al.* 2000; Maeder *et al.* 2001; Pirozzoli *et al.* 2004; Duan 2011; Pirozzoli & Bernardini 2011) and internal flows (Huang *et al.* 1995). Guarini *et al.* (2000) showed via a thorough analysis that HSRA revealed a key analogy between the normalized rates of turbulent heat and momentum transfers. In the present paper, we prove that this key analogy, and hence HSRA, are a consequence of the GRA, which is an advance since HSRA was proposed phenomenologically (Gaviglio 1987; Huang *et al.* 1995). A slight modification to HSRA is also suggested by the GRA, and this agrees with DNS better than HSRA. These findings are obtained by considering the deviation from real turbulence of the strong analogy assumption of the SRA (for zero-pressure-gradient adiabatic CTBLs, assumption *b* given above). As will be shown, this deviation can be utilized to explain the reason for the validity of HSRA and the variation of the temperature–velocity correlation coefficient with wall temperature.

This paper presents the theory of the GRA, its validation, and application. The paper is structured as follows. The DNS cases used for assessing the GRA and the other Reynolds analogy theories are briefly described in § 2. The existing Reynolds analogy theories are reviewed and analysed in § 3. The GRA is derived in § 4, followed by the results on the mean temperature–velocity relationship in § 5 and the fluctuation

temperature–velocity relationship in § 6. Discussions appear in § 7 and conclusions in § 8. Appendices give derivations of some important formulae.

2. DNS for assessing the Reynolds analogy theories

We assess the GRA and the other Reynolds analogy theories using the DNS data listed in table 1. The DNS were carried out by several groups and on different flows, including Ghosh, Foysi & Friedrich (2010) for CPF and CCF, Huang *et al.* (1995) for CCFs, Duan (2011) for CTBLs, Wang (2012) for CCFs, and Pirozzoli & Bernardini (2011) and us for CTBLs that employ a spatially evolving simulation. The DNS of Wang and ours have used the code developed by Xin-Liang Li with numerical details documented in Li, Ma & Fu (2001) for CCFs and Li, Fu & Ma (2006) for CTBLs. In table 1, notation CPFM1.30Θ − 0.77, for example, denotes a CPF at $M = 1.30$ and $\Theta = -0.77$. Here the M for external and internal flows, respectively, are defined as $M_\infty = \bar{u}_\infty/\sqrt{\gamma R\bar{T}_\infty}$ (Duan 2011) and $M_m = \bar{u}_m/\sqrt{\gamma R\bar{T}_w}$ (Ghosh *et al.* 2010), where subscript ∞ denotes free stream and subscript m means averaged in the pipe/channel cross-section. $\Theta = (\bar{T}_w - \bar{T}_\delta)/(\bar{T}_r - \bar{T}_\delta)$ is a dimensionless wall temperature that we call the diabatic parameter. Θ is calculated by using the recovery temperature $\bar{T}_r \equiv \bar{T}_\delta + r\bar{u}_\delta^2/(2C_p)$ with the recovery factor $r = 0.9$ for all the DNS. In CCFs/CPFs δ denotes the channel/pipe centre. Note that the DNS cases in table 1 cover adiabatic/diabatic walls, with/without pressure gradients and both external and internal flows. The parameter space is also broad, and consists of Reynolds number ($Re_\tau = 220 \sim 2100$), Mach number ($M = 2.00 \sim 9.40$) and the diabatic parameter ($\Theta = -1.01 \sim 1.00$).

3. A review of the Reynolds analogy theories

The time-averaged Navier–Stokes equations are (Gatski & Bonnet 2009)

$$\partial_{x_i}(\overline{\rho u_i}) = 0, \tag{3.1}$$

$$\partial_{x_j}(\overline{\rho u_i u_j}) = -\partial_{x_i}\bar{p} + \partial_{x_j}(\overline{\tau_{x_i x_j}}), \tag{3.2}$$

$$\partial_{x_j}(\overline{\rho u_j H}) = \partial_{x_j}(\overline{u_i \tau_{x_i x_j}}) - \partial_{x_j}(\overline{q_{x_j}}), \tag{3.3}$$

where (3.1)–(3.3) are the continuity, momentum, and energy equations, ρ is density, p is pressure, $H = C_pT_t = h + u_iu_i/2$ is total enthalpy, $h = C_pT$ is enthalpy, $\tau_{x_ix_j} = 2\mu(S_{ij} - S_{kk}\delta_{ij}/3)$ is the viscous stress tensor with $S_{ij} = (\partial_{x_j}u_i + \partial_{x_i}u_j)/2$, $q_{x_i} = -k\partial_{x_i}T$ is heat flux, μ is viscosity that is related to thermal conductivity k by $Pr = C_p\mu/k$. In this paper the following approximations are frequently adopted:

$$u_iu_i \approx u^2, \quad u^2 \approx \bar{u}^2 + 2\bar{u}u', \tag{3.4}$$

which are called the quasi-parallel flow approximation and the small turbulence intensity approximation, respectively. They are both rather accurate and widely applied in the analysis of canonical CWTFs. For convenience, the review in this section is limited to zero-pressure-gradient CTBLs.

3.1. *Crocco–Busemann relation (1931, 1932), SRA (1962), and extended SRA (1974)*

Owing to Young's work in 1951 (Howarth 1953; Spina, Smits & Robinson 1994), the energy equation can be written in the form of total enthalpy (Gatski & Bonnet 2009):

$$\begin{aligned}\bar{\rho}\bar{u}\partial_x\bar{H} + \bar{\rho}\bar{v}\partial_y\bar{H} = {} & \partial_y[(\bar{\mu}/Pr)\partial_y\bar{H} - \overline{\rho H'v'}] \\ & + \partial_y[\bar{\mu}(1 - 1/Pr)\partial_y(\bar{u}_i\bar{u}_i/2 - \overline{u_i'u_i'}/2)].\end{aligned} \tag{3.5}$$

https://doi.org/10.1017/jfm.2013.620 Published online by Cambridge University Press

Case	Re_τ	Case	Re_τ
CPFM1.30Θ − 0.77 (Ghosh2010)	245	CCFM6.00Θ − 0.97 (Wang2012)	987
CCFM1.26Θ − 0.94 (Ghosh2010)	246	CCFM6.00Θ − 1.01 (Wang2012)	1536
CCFM1.50Θ − 0.71 (Huang1995)	220	CTBLM2.00Θ1.00 (Pirozzoli2011)	1116 (205 ∼ 1123 in DNS)
CCFM3.00Θ − 0.72 (Huang1995)	448	CTBLM2.25Θ0.99	550 (500 ∼ 1000 in DNS)
CCFM1.50Θ − 0.54 (Wang2012)	430	CTBLM4.50Θ0.93	550 (325 ∼ 600 in DNS)
CCFM3.00Θ − 0.71 (Wang2012)	431	CTBLM4.50Θ0.41	800 (600 ∼ 860 in DNS)
CCFM3.00Θ − 0.75 (Wang2012)	693	CTBLM4.50Θ0.00	2100 (1950 ∼ 2350 in DNS)
CCFM3.00Θ − 0.78 (Wang2012)	918	CTBLM6.00Θ0.92	550 (275 ∼ 600 in DNS)
CCFM6.00Θ − 0.73 (Wang2012)	430	CTBLM3.40 ∼ 9.40Θ 0.60 ∼ −0.29 (Duan2011)	377, 398, . . . , 938

TABLE 1. The DNS used for assessing the Reynolds analogy theories. Data taken from Ghosh *et al.* (2010), Huang *et al.* (1995), Duan (2011), Wang (2012), and from Pirozzoli & Bernardini (2011) and our DNS that employ a spatially evolving simulation.

If $Pr = 1$, the momentum and energy equations would display a similarity to give

$$\bar{\rho}\bar{u}\partial_x\bar{u} + \bar{\rho}\bar{v}\partial_y\bar{u} = \partial_y(\bar{\mu}\partial_y\bar{u} - \overline{\rho u'v'}), \tag{3.6}$$

$$\bar{\rho}\bar{u}\partial_x\bar{H} + \bar{\rho}\bar{v}\partial_y\bar{H} = \partial_y(\bar{\mu}\partial_y\bar{H} - \overline{\rho H'v'}). \tag{3.7}$$

To find an analogy solution of (3.6) and (3.7), a 'strong' analogy assumption has been introduced:

$$H' = U_w u', \tag{3.8}$$

where U_w is a proportionality constant with dimension of velocity. Subtracting (3.6) from (3.7) gives

$$(\bar{\rho}\bar{u}\partial_x + \bar{\rho}\bar{v}\partial_y - \partial_y(\bar{\mu}\partial_y))(\bar{H} - U_w\bar{u}) = 0, \tag{3.9}$$

whose solution is

$$\bar{H} - \bar{H}_w = U_w\bar{u}, \tag{3.10}$$

where $\bar{H}_w$ is the total enthalpy at the wall and $U_w = -\bar{q}_{yw}/\bar{\tau}_w$. The mean temperature–velocity relation can be derived from (3.10), as

$$\frac{\bar{T}}{\bar{T}_\delta} = \frac{\bar{T}_w}{\bar{T}_\delta} + \frac{\bar{T}_{t\delta} - \bar{T}_w}{\bar{T}_\delta}\frac{\bar{u}}{\bar{u}_\delta} + \frac{\bar{T}_\delta - \bar{T}_{t\delta}}{\bar{T}_\delta}\left(\frac{\bar{u}}{\bar{u}_\delta}\right)^2, \quad \bar{T}_{t\delta} = \bar{T}_\delta + \frac{\bar{u}_\delta^2}{2C_p}. \tag{3.11}$$

Equation (3.11) is called the Crocco–Busemann relation since it is similar to the relation derived by Busemann (1931) and Crocco (1932) for compressible laminar boundary layers.

In the case of an adiabatic wall, $\bar{q}_{yw} = 0$ gives $U_w = 0$. The strong analogy solutions become $\bar{T}_t = \bar{T}_w$ and $T_t' = 0$. The former has been moderately well confirmed by DNS (Guarini *et al.* 2000), which shows the mean total temperature to deviate from a constant value by less than 7 % for an $M = 2.5$ CTBL. The latter leads to

$$T' + (\bar{u}/C_p)u' = 0. \tag{3.12}$$

This instantaneous relation has several statistical consequences: $\overline{u'T'} = -(\bar{u}/C_p)\overline{u'^2}$, $\sqrt{\overline{T'^2}} = (\bar{u}/C_p)\sqrt{\overline{u'^2}}$, and $\overline{\rho T'v'} = -(\bar{u}/C_p)\overline{\rho u'v'}$, and also

$$\frac{\sqrt{\overline{T'^2}}/\bar{T}}{(\gamma - 1)M^2\sqrt{\overline{u'^2}}/\bar{u}} = 1, \tag{3.13}$$

$$R_{u'T'} = \frac{\overline{u'T'}}{\sqrt{\overline{u'^2}}\sqrt{\overline{T'^2}}} = -1, \tag{3.14}$$

$$Pr_t = \frac{\overline{\rho u'v'}(\partial\bar{T}/\partial y)}{\overline{\rho T'v'}(\partial\bar{u}/\partial y)} = 1, \tag{3.15}$$

$$\frac{\sqrt{\overline{T'^2}}}{\bar{T}_w - \bar{T}_\delta} = 2\frac{\bar{u}}{\bar{u}_\delta}\frac{\sqrt{\overline{u'^2}}}{\bar{u}_\delta}. \tag{3.16}$$

In (3.13), $M = \bar{u}/\sqrt{\gamma R\bar{T}}$. Equations (3.12)–(3.16) identified by Morkovin (1962) are collectively known as the *strong Reynolds analogy*.

The assumption of negligible T_t' (i.e. (3.12)) was invalidated by both experiment (Debieve, Gouin & Gaviglio 1982; Gaviglio 1987) and DNS (Guarini *et al.* 2000; Maeder *et al.* 2001; Duan, Beekman & Martín 2011). They showed that $\sqrt{\overline{T_t'^2}}$ is

comparable to $\sqrt{\overline{T'^2}}$. Consequently, the SRA relations are generally poorly satisfied. For example, the predictions of $R_{u'T'} = -1$ and $Pr_t = 1$ clearly deviate from the observed values of $R_{u'T'} = -0.7 \sim -0.5$ and $Pr_t = 0.7 \sim 0.9$ in quasi-adiabatic CTBLs up to the hypersonic regime (Guarini *et al.* 2000; Maeder *et al.* 2001; Pirozzoli *et al.* 2004; Duan 2011; Pirozzoli & Bernardini 2011). However, (3.13) is well satisfied in both experiments (Gaviglio 1987) and numerical simulations (Guarini *et al.* 2000). Then a question arises as to why (3.13) is satisfied under an incorrect assumption. Regarding this, both Debiève (1976) and Gaviglio (1987) demonstrated that (3.12) is a sufficient but not necessary condition of (3.13). By rearranging the r.m.s. of the total temperature fluctuations as

$$\frac{\sqrt{\overline{T'^2} - \overline{T_t'^2} + 2\overline{T_t'T'}}/\bar{T}}{(\gamma - 1)M^2\sqrt{\overline{u'^2}}/\bar{u}} = 1, \tag{3.17}$$

Guarini *et al.* (2000) pointed out that the validity of (3.13) came from $\overline{T'^2} \gg \overline{T_t'^2} - 2\overline{T_t'T'}$, instead of $\overline{T_t'^2} = 0$. Gaviglio (1987) noticed that the total temperature fluctuation could be written in a general form as

$$\sqrt{\overline{T_t'^2}} = \left[\overline{T'^2} + \overline{u'^2}(\bar{u}/C_p)^2 + 2(\bar{u}/C_p)\sqrt{\overline{u'^2}}\sqrt{\overline{T'^2}}R_{u'T'}\right]^{1/2}. \tag{3.18}$$

Applying (3.13)–(3.18), one obtains $R_{u'T'} = \overline{T_t'^2}/(2\overline{T'^2}) - 1$ (Gaviglio 1987), which performs better than (3.14).

SRA can be extended to diabatic flows. Substituting $\bar{T}_{t\delta} - \bar{T}_w = \bar{u}_\delta(U_w/C_p)$ into the assumption $H' = U_w u'$, with the approximations in (3.4), one obtains

$$-\frac{T'/\bar{T}}{(\gamma - 1)\,M^2 u'/\bar{u}} = 1 - C_p\frac{\bar{T}_{t\delta} - \bar{T}_w}{\bar{u}_\delta \bar{u}}, \tag{3.19}$$

$$\frac{\sqrt{\overline{T'^2}}/\bar{T}}{(\gamma - 1)\,M^2\sqrt{\overline{u'^2}}/\bar{u}} = 1 - C_p\frac{\bar{T}_{t\delta} - \bar{T}_w}{\bar{u}_\delta \bar{u}}. \tag{3.20}$$

The instantaneous relationship (3.19) was proposed by Cebeci & Smith (1974), and the r.m.s. form of (3.19), i.e. (3.20), was suggested as an extended SRA by Gaviglio (1987). In the case when there is heat flux at the wall, the extended SRA is a noteworthy improvement over the SRA, but the deviation from real turbulence is still noticeable (Gaviglio 1987).

3.2. *Walz's equation (1962)*

The deviation of Pr from unity is one of the reasons responsible for the difference between DNS and Crocco–Busemann relation, which was modified later by Walz (1962). Walz presented an approximate solution of the Reynolds-averaged Navier–Stokes equations with the assumption of constant mixed Prandtl number, i.e. $Pr_m =$ const, which is a reasonable approximation for CTBLs and other shear flows (Smits & Dussauge 2006). Pr_m is defined by $Pr_m = C_p(\bar{\mu} + \bar{\mu}_t)/(\bar{k} + \bar{k}_t)$, where $\bar{\mu}_t = (-\overline{\rho u'v'})/(\partial\bar{u}/\partial y)$ is eddy viscosity and $\bar{k}_t = (-C_p\overline{\rho T'v'})/(\partial\bar{T}/\partial y)$ is eddy thermal conductivity.

In Walz's derivation, temperature is assumed a function of only u, and the Reynolds-averaged Navier–Stokes equations are written in terms of the independent variables x and u, instead of x and y. After neglecting most streamwise derivatives, the energy

equation can be written (Walz 1966; Smits & Dussauge 2006)

$$\bar{\tau}\left[\partial_{\bar{u}}(\partial_{\bar{u}}\bar{T}/Pr_m)+1/C_p\right]+(1/Pr_m-1)\partial_{\bar{u}}\bar{T}\partial_{\bar{u}}\bar{\tau}=0, \tag{3.21}$$

where $\bar{\tau}$ is the total shear stress. The boundary conditions are (a) $\bar{u}=0:\bar{T}=\bar{T}_w$, $(\partial\bar{\tau}/\partial y)_{y=0}=\mathrm{d}p/\mathrm{d}x=0$; (b) $\bar{u}=\bar{u}_\delta:\bar{T}=\bar{T}_\delta,\bar{\tau}=\bar{\tau}_\delta=0$. With the assumption $Pr_m=$ const, (3.21) can be integrated two times to obtain

$$\frac{\bar{T}}{\bar{T}_\delta}=\frac{\bar{T}_w}{\bar{T}_\delta}+\frac{\bar{T}_r-\bar{T}_w}{\bar{T}_\delta}f_1+\frac{\bar{T}_\delta-\bar{T}_r}{\bar{T}_\delta}f_2, \tag{3.22}$$

where f_1,f_2 and r in Tr are functions of $\bar{\tau}/\bar{\tau}_w$, Pr_m and $\bar{u}/\bar{u}_\delta$ (Walz 1966). Using a linear approximation $\bar{\tau}/\bar{\tau}_w=1-y/\delta$ and $Pr_m=0.86$ averaged over the boundary layer, Walz (1966) found that $f_1=\bar{u}/\bar{u}_\delta$, $f_2=(\bar{u}/\bar{u}_\delta)^2$ and $r=0.88$. Then, (3.22) has the same form as (3.11), and was called the modified Crocco–Busemann relation or Walz's equation.

Here we notice that Walz's equation can be rewritten as

$$\bar{H}_r-\bar{H}_w=U_w\bar{u}, \tag{3.23}$$

where $\bar{H}_r=C_p\bar{T}_{ry}$ is a *local* recovery enthalpy and $\bar{T}_{ry}=\bar{T}+r\bar{u}^2/(2C_p)$ is a *local* recovery temperature, $U_w=-Pr\bar{q}_{yw}/\bar{\tau}_w$. The emphasis on local here is to distinguish $\bar{T}_{ry}$ from $\bar{T}_r$. Comparing with (3.10), (3.23) suggests an analogy between local excess recovery enthalpy and velocity.

3.3. *Modified SRAs (1987, 1990, 1995, 2008)*

Gaviglio (1987) attempted to establish a relationship between u' and T' based on the dominant role of the large-scale motion in CWTFs. He proposed that the fluctuating velocity and temperature induced by the large-scale movements are proportional to the local gradient of mean velocity and temperature, which gives $aT'/\partial_y\bar{T}=u'/\partial_y\bar{u}$ and $a\sqrt{\overline{T'^2}}/\partial_y\bar{T}=\sqrt{\overline{u'^2}}/\partial_y\bar{u}$ with a being the ratio of the velocity mixing length $\ell_u=\sqrt{\overline{u'^2}}/(\partial\bar{u}/\partial y)$ over the temperature mixing length $\ell_T=\sqrt{\overline{T'^2}}/(\partial\bar{T}/\partial y)$. Based on experimental data, Gaviglio assumed $a=1$ to obtain (1.2). Rubesin (1990) independently gave an equivalent form of (1.2) with a associated with some turbulence modelling constants. Huang *et al.* (1995) showed that a should be equal to Pr_t. Indeed, multiplying both sides of $aT'/\partial_y\bar{T}=u'/\partial_y\bar{u}$ by $\rho v'$ and averaging, one obtains $a=(\overline{\rho v'u'}\partial_y\bar{T})/(\overline{\rho v'T'}\partial_y\bar{u})=Pr_t$, which gives the HSRA. In a recent work by Brun *et al.* (2008), a was modelled to be $1/Pr_m$ for channels.

HSRA works well for canonical CWTFs under different wall conditions. In channel flows over cold walls, Huang *et al.* (1995) showed that HSRA is an improvement over the extended SRA. In CTBLs, Duan's DNS up to $M=12$ showed that HSRA is effective for adiabatic and diabatic, catalytic and non-reacting walls under low- and high-enthalpy conditions (Duan 2011).

3.4. *The empirical relation of Duan & Martín (2011)*

Recently, Duan & Martín (2011) successfully removed the explicit dependence of the mean temperature–velocity relationship on the thermal and chemical wall conditions with an empirical relation, in which a dimensionless excess recovery enthalpy $\bar{H}_r^*=(\bar{H}_r-\bar{H}_w)/(\bar{H}_{r\delta}-\bar{H}_w)$ is defined. For a calorically perfect gas, $\bar{H}_r^*$ reduces to a dimensionless excess recovery temperature: $T_{ry}^*=(\bar{T}_{ry}-\bar{T}_w)/(\bar{T}_{r\delta}-\bar{T}_w)$. By plotting $\bar{T}_{ry}^*$ versus $\bar{u}/\bar{u}_\delta$, they found that all the DNS data collapse, independently of the

free-stream Mach number, wall temperature, surface catalysis and enthalpy conditions. The best fitting of $\bar{T}^*_{ry} = f(\bar{u}/\bar{u}_\delta)$ gives

$$f\left(\frac{\bar{u}}{\bar{u}_\delta}\right) = (1-\alpha)\left(\frac{\bar{u}}{\bar{u}_\delta}\right)^2 + \alpha\left(\frac{\bar{u}}{\bar{u}_\delta}\right), \quad \alpha = 0.8259. \tag{3.24}$$

By expanding the equation $\bar{T}^*_{ry} = f(\bar{u}/\bar{u}_\delta)$, Duan & Martín (2011) obtained a mean temperature–velocity relationship:

$$\frac{\bar{T}}{\bar{T}_\delta} = \frac{\bar{T}_w}{\bar{T}_\delta} + \frac{\bar{T}_r - \bar{T}_w}{\bar{T}_\delta} f\left(\frac{\bar{u}}{\bar{u}_\delta}\right) + \frac{\bar{T}_\delta - \bar{T}_r}{\bar{T}_\delta}\left(\frac{\bar{u}}{\bar{u}_\delta}\right)^2. \tag{3.25}$$

The only difference between (3.25) and Walz's equation (3.22) is that $\bar{u}/\bar{u}_\delta$ in the second term of the right-hand side of Walz's equation is replaced by $f(\bar{u}/\bar{u}_\delta)$.

3.5. *A few remarks*

We recall here the key approximations and assumptions involved in the previous Reynolds analogy theories, which result in the final differences between the theories and the real turbulence. In the Crocco–Busemann relation, SRA and the extended SRA, the approximation $Pr = 1$ and the assumption $H' = U_w u'$ are introduced. Both are not good descriptions of the real turbulence. Young pointed out that the difference caused by $Pr \neq 1$ *represents a measurement of the dissimilarity of the two different modes of transfer for vector* $\rho\boldsymbol{u}$ *and scalar* T_t *which do not respond in the same manner to change in density and pressure* (Gaviglio 1987). The assumption $H' = U_w u'$ is an 'exact' analogy, too strong to be met in real turbulence. A consequence of this equation of instantaneous fluctuations is the rigorous relation $|R_{u'T'}| = 1$, which is invalid in real turbulence.

Two key approximations are made to derive Walz's equation: (*a*) $Pr_m = \text{const}$; (*b*) $\bar{\tau}/\bar{\tau}_w = 1 - y/\delta$. Since f_1, f_2 and r are complex functions of Pr_m and $\bar{\tau}/\bar{\tau}_w$, it is difficult to quantify the error introduced by the two approximations, especially (*b*). However, our DNS data show that: (i) for quasi-adiabatic CTBLs, $1 - \bar{\tau}/\bar{\tau}_w = (y/\delta)^n$ with $n \approx 1.35$ at $M = 2.25$ and $n \approx 1.10$ at $M = 6.00$; (ii) for diabatic CTBLs, the performance of approximation (*b*) becomes worse.

All in all, an improved theory should avoid, if possible, those approximations and assumptions that are inconsistent with actual turbulence physics. Also, this improved theory would be better proposed based on the conservation laws, instead of schematic or phenomenological models like some modified SRAs. Deriving successful relations (such as those of Duan & Martín 2011 and Huang *et al.* 1995) is another target of an improved theory, since many flow properties have been captured by these formulae. In the next section, we present a generalized Reynolds analogy that we believe to meet the above requirements.

4. Generalized Reynolds analogy

4.1. *Generalized Reynolds analogy as a formal generalization of the SRA*

We now give a derivation of the GRA as a formal generalization of the SRA. In the case of zero pressure gradient and unity Prandtl number, the SRA finds that the Reynolds-averaged momentum and energy equations of CTBLs are similar and admit the solution

$$\bar{H} - \bar{H}_w = U_w \bar{u}, \tag{4.1}$$

$$H' = U_w u'. \tag{4.2}$$

For $Pr \neq 1$, different molecular momentum and thermal transports lead to differing velocity and temperature fields. In air flow over an adiabatic wall without pressure gradient, the Prandtl number of 0.7 results in a temperature deficiency in the wall vicinity, which is accounted for in Walz's equation using the recovery factor r of $\sim$0.9. In other words, it is the local recovery enthalpy, rather than the total enthalpy, that approximately keeps constant in the shear region, i.e. (3.23) with $U_w = 0$. Based on these observations, we introduce a general recovery factor r_g to account for the effect of $Pr \neq 1$ in flows over diabatic walls, and assume a formal generalization of (4.1) as

$$\bar{H}_g - \bar{H}_w = U_w \bar{u}, \tag{4.3}$$

where $H_g \equiv C_p T + r_g u^2/2$ is a general recovery enthalpy, and $U_w = -Pr\bar{q}_{yw}/\bar{\tau}_w$. Note that r_g is a mean-field quantity that, in general, varies with the wall-normal coordinate, and (4.3) and its wall-normal derivative equation are valid at the wall independent of r_g. We can also define a general recovery temperature T_{rg} so that $H_g = C_p T_{rg}$. For an adiabatic wall condition and assuming $r_g = r$, (4.3) leads to Walz's equation.

The problem with (4.2) is that this 'strong' analogy can hardly be satisfied in real turbulence. For an adiabatic flow, (4.2) predicts a negligible total temperature fluctuation intensity, clearly invalid (Guarini *et al.* 2000; Maeder *et al.* 2001; Duan *et al.* 2011). Therefore, we introduce for the general recovery enthalpy fluctuations:

$$H_g' + C_p \phi' = U_w u', \tag{4.4}$$

where $H_g' = C_p T_{rg}' = C_p T' + r_g \bar{u} u'$, with a residual temperature ϕ' that is the instantaneous difference between T_{rg}' and $(U_w/C_p)u'$ in real turbulence. The introduction of ϕ' remedies the contradiction of (4.2) for adiabatic flows: when $U_w = 0$, $T_{rg}' = -\phi'$. With a non-negligible ϕ', one can describe a non-zero T_{rg}' in adiabatic flows.

Now, we determine r_g by considering the turbulent momentum and thermal transport, which occurs mainly in the wall-normal direction. Multiplying (4.4) by $(\rho v)'$ and averaging, r_g is solved as

$$r_g = \frac{C_p}{\bar{u}} \left[\frac{U_w}{C_p} - \frac{\overline{(\rho v)' T'}}{\overline{(\rho v)' u'}} - \frac{\overline{(\rho v)' \phi'}}{\overline{(\rho v)' u'}} \right]. \tag{4.5}$$

Equation (4.5) can further be written as

$$r_g = \frac{C_p}{\bar{u}} \left[\left. \frac{\partial \bar{T}}{\partial \bar{u}} \right|_w - \frac{1}{\overline{Pr_e}} \frac{\partial \bar{T}}{\partial \bar{u}} \right], \tag{4.6}$$

where

$$\overline{Pr_e} \equiv \frac{\overline{Pr_t}}{1 + \varepsilon}, \tag{4.7}$$

$$\overline{Pr_t} \equiv \frac{\overline{(\rho v)' u'}}{\overline{(\rho v)' T'}} \frac{\partial \bar{T}/\partial y}{\partial \bar{u}/\partial y}, \tag{4.8}$$

and $\varepsilon = (\overline{(\rho v)' \phi'}/\overline{(\rho v)' T'})$. $\overline{Pr_e}$ is called an effective turbulent Prandtl number and $\overline{Pr_t}$ is a new turbulent Prandtl number. Note that $\overline{Pr_t}$ is different from the classical definition of $Pr_t \equiv (\overline{\rho v' u'}/\overline{\rho v' T'})((\partial \bar{T}/\partial y)/(\partial \bar{u}/\partial y))$: $\overline{Pr_t} = Pr_t(1 + \bar{v}\overline{\rho' u'}/\overline{\rho v' u'})/(1 + \bar{v}\overline{\rho' T'}/\overline{\rho v' T'})$, which results in a quantitative difference between $\overline{Pr_t}$ and Pr_t in CTBLs where both $\bar{v}$ and ρ' are non-zero. We will address this quantitative difference later

on. In an adiabatic flow, $\varepsilon = -\overline{(\rho v)'T'_{rg}}/\overline{(\rho v)'T'}$, which is the ratio between the wall-normal turbulent transfer of the general recovery energy to the wall-normal heat flux. Morkovin (1962) assumed that $\overline{(\rho v)'T'_t}$ is much smaller than $\overline{(\rho v)'T'}$, found to be only approximately valid near the wall (Guarini *et al.* 2000). Thus, we can deduce that ε is generally not negligible.

Substitution of (4.6) into (4.3) gives the differential equation for the mean temperature:

$$\bar{T} - \frac{\bar{u}}{2}\left[\left.\frac{\partial \bar{T}}{\partial \bar{u}}\right|_w + \frac{1}{\overline{Pr_e}}\frac{\partial \bar{T}}{\partial \bar{u}}\right] = \bar{T}_w. \tag{4.9}$$

Equation (4.9) shows that $\overline{Pr_e}$ determines the profile of mean temperature versus mean velocity, which is the reason why we call $\overline{Pr_e}$ the effective turbulent Prandtl number. Similarly, the relationship between T' and u' can be derived by substituting (4.5) into (4.4), yielding

$$T' - \frac{1}{\overline{Pr_t}}\frac{\partial \bar{T}}{\partial \bar{u}}u' + \phi' - \frac{\overline{(\rho v)'\phi'}}{\overline{(\rho v)'u'}}u' = 0. \tag{4.10}$$

So far, by formally generalizing the SRA, we have proposed a possible Reynolds analogy between the excess general recovery enthalpy and the streamwise velocity for compressible wall-bounded turbulence with arbitrary Prandtl number and with heat flux at the wall. This proposal, that we call the generalized Reynolds analogy, consists of (4.3), (4.4) and (4.6) (or (4.5)), with ϕ' to be determined by invoking additional models. In the next section, the GRA is validated as a solution of the Reynolds-averaged momentum and energy equations of CWTFs.

4.2. *Validation of the generalized Reynolds analogy*

In this validation, we restrict our analysis to the CWTFs that satisfy the quasi-parallel-flow approximation and the low-turbulence-intensity approximation expressed by (3.4), and the small-streamwise-derivative approximation that is widely applied in boundary layer theory. These approximations can be concluded to be the quasi-one-dimensional flow approximation that is valid for the canonical CWTFs such as CCFs, CPFs, and CTBLs with moderate pressure gradients. Applying these approximations, the Reynolds-averaged streamwise momentum equation and energy equation of a CWTF can be written as (see appendix A)

$$\overline{\rho u}\partial_x \bar{u} + \overline{\rho v}\partial_y \bar{u} = -\partial_x \bar{p} + \partial_y[\bar{\mu}\partial_y \bar{u} - \overline{(\rho v)'u'}], \tag{4.11}$$

$$\overline{\rho u}\partial_x \bar{H} + \overline{\rho v}\partial_y \bar{H} = \partial_y[\bar{u}\bar{\mu}\partial_y \bar{u} - \overline{(\rho v)'H'} - \bar{q}_y]. \tag{4.12}$$

By using the relation

$$H = H_g + (1 - r_g)u^2/2, \tag{4.13}$$

equation (4.12) can be rearranged as (see appendix B)

$$\overline{\rho u}\partial_x(\bar{H}_g) + \overline{\rho v}\partial_y(\bar{H}_g) = \partial_y[\bar{\mu}\partial_y(\bar{H}_g) - \overline{(\rho v)'H'_g}] + f(r_g), \tag{4.14}$$

where $f(r_g)$ contains all the rest of the terms. For the GRA to be a solution, (4.14) should have been written in the following similar form:

$$\overline{\rho u}\partial_x(\bar{H}_g) + \overline{\rho v}\partial_y(\bar{H}_g) = -U_w\partial_x \bar{p} + \partial_y[\bar{\mu}\partial_y(\bar{H}_g) - \overline{(\rho v)'(H'_g + C_p\phi')}], \tag{4.15}$$

which is equivalent to

$$f(r_g) = -U_w \partial_x \bar{p} - C_p \partial_y \overline{(\rho v)' \phi'}. \tag{4.16}$$

Equation (4.16) can be proved by applying the GRA relations (4.3), (4.4) and (4.6), as shown in detail in appendix B.

Thus, we are able to derive, in a self-consistent way, similar forms of the Reynolds-averaged momentum and energy equations for the CWTF. The similarity between (4.11) and (4.15) admits the solution expressed by the GRA relations. Note that the similarity between the turbulent terms in (4.11) and (4.15) is different from what is usually written: an additional ϕ' is included in (4.15). We prefer Guarini *et al.*'s (2000) viewpoint that (4.4) enables elimination of the turbulent terms to solve (4.3). In other words, (4.4) implies (4.3). Another note is that the CWTF treated above is not restricted to specific Prandtl number, wall temperature and streamwise pressure gradient (provided that the quasi-one-dimensional flow approximation is satisfied), so the GRA solution is rather general.

5. GRA relationship between mean temperature and mean velocity

Now we study the GRA relationship between mean temperature and mean velocity. Equation (4.9) can be integrated if $\overline{Pr_e}$ is a known function of $\bar{T}$ and $\bar{u}$. By calculating the derivative of (4.9) at the wall (with respect to $\bar{u}$), we find that $\overline{Pr_e}$ equals one at the wall independent of flow conditions (see also (5.5)). Furthermore, for r_g to be a finite number at the wall, $\bar{T}$ is a quadratic function of $\bar{u}$ in the wall vicinity owing to (4.6), formally agreeing with the Crocco–Busemann relation and Walz's equation. Consequently, it is tempting to adopt the simplest model for $\overline{Pr_e}$ and assume

$$\overline{Pr_e} = 1 \tag{5.1}$$

across the boundary layer and invariant to flow conditions. We assess (5.1) by using the DNS of Pirozzoli & Bernardini (2011) and our DNS for CTBLs. Because ϕ' in the definition of $\overline{Pr_e}$ is unknown yet, $\overline{Pr_e}$ can only be inversely calculated by using (4.9). As shown in figure 1(*a*), $\overline{Pr_e}$ is within 1.0 ± 0.1 in most of the CTBLs without a mild dependence on M, Re and wall temperature condition. There are clear deviations above $\sim 0.85\delta$, which approximates the lower edge of the entrainment/intermittent region (Zhang *et al.* 2012). Since the flow there is not fully turbulent, this deviation is not unexpected. Fortunately, because the mean velocity profile is quite constant in the entrainment/intermittent region, the deviation of $\overline{Pr_e}$ from unity has a negligible effect on the relationship between the mean temperature and the mean velocity integrated through (4.9) under the assumption (5.1). In the very near-wall region of cooled CTBLs, $\overline{Pr_e}$ diverges and has a sign transition near the location where the mean temperature peaks, so that $\overline{Pr_e}$ significantly deviates from unity there. The divergence is because the locations of $\overline{(\rho v)' T'} = 0$ and $\partial \bar{T}/\partial y = 0$ are slightly different. Although the DNS show that $\overline{Pr_e}$ varies a lot near the wall, as will be shown we can smooth this divergent $\overline{Pr_e}$ with (5.1) without noticeably affecting the mean temperature–velocity relationship integrated through (4.9).

An important issue with the testing of the assumption $\overline{Pr_e} = 1$ in diabatic CTBLs is to reveal the thickness of the zone influenced by wall cooling: it is a real test when this thickness is large enough to be comparable to the boundary layer thickness. To do this, we define the thickness of the zone influenced by wall cooling/heating as $\delta_{\hat{T}} : |\bar{T}_{\delta_{\hat{T}}-adiabatic} - \bar{T}_{\delta_{\hat{T}}-diabatic}|/(\bar{T}_{w-adiabatic} - \bar{T}_\infty) = 1\,\%$, where $\bar{T}_{\delta_{\hat{T}}-adiabatic}$ is the mean temperature at $\delta_{\hat{T}}$ for an adiabatic flow; $\delta_{\hat{T}}$ is a measure of the thickness of the

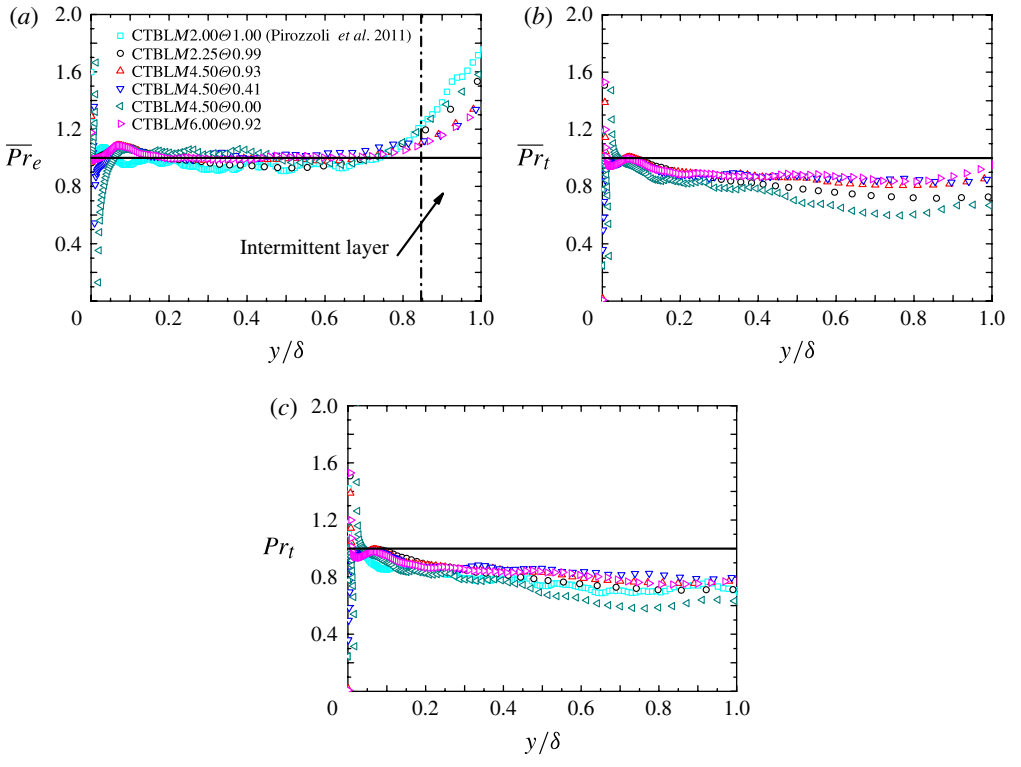

FIGURE 1. (Colour online) Profiles of (*a*) $\overline{Pr_e}$, (*b*) $\overline{Pr_t}$ and (*c*) Pr_t for fully developed CTBLs at different Mach numbers, Reynolds numbers and under different wall temperature conditions.

zone where the adiabatic mean temperature profile is noticeably reduced to a diabatic mean temperature profile by wall cooling. Thus, we can measure that $\delta_{\hat{T}}$ is 1.056δ for the case CTBLM4.50Θ0.00. Therefore, the assumption $\overline{Pr_e} = 1$ is assessed to be independent of wall temperatures.

In figures 1(*b*) and 1(*c*), the profiles of $\overline{Pr_t}$ and Pr_t are plotted for comparison with those of $\overline{Pr_e}$; $\overline{Pr_t}$ is different from Pr_t only in the outer regions of CTBLs at large Mach numbers, which we will address later on. Pr_t varies in the range of $0.6 \sim 0.9$, in accordance with the previous studies (Pirozzoli *et al.* 2004; Duan *et al.* 2011). Because $Pr_t \approx \overline{Pr_t} = \overline{Pr_e}(1+\varepsilon) \approx 1+\varepsilon$, the discrepancy between Pr_t and one is due to $\varepsilon(= \overline{(\rho v)'\phi'}/\overline{(\rho v)'T'})$ being both negative and non-negligible in the bulk region. In the adiabatic flow, especially, $\varepsilon = -\overline{(\rho v)'T'_{r_g}}/\overline{(\rho v)'T'}$ so that $Pr_t \approx 1 - (\overline{(\rho v)'T'_{r_g}}/\overline{(\rho v)'T'})$. Therefore, we conclude that the mean fields of temperature and streamwise velocity are determined universally by a unity turbulent Prandtl number, which is $\overline{Pr_e}$ (figure 1*a*). In contrast, the classical turbulent Prandtl number Pr_t is systematically changed from unity by the residue temperature ϕ' that is the deviation from the 'exact' analogy relation of the fluctuation fields. In this regard, we reveal that the mean fields are more stable to flow conditions, whereas Pr_t is a complex function of flow parameters such as Pr, Re, pressure gradient, surface roughness, wall blowing and suction, etc. (Kays 1994). Finally, for the same reason as that of $\overline{Pr_e}$, a divergence is observed in the near-wall profile of Pr_t, found also in Duan (2011).

With the assumption (5.1), (4.9) can be integrated analytically to give the GRA relationship between mean temperature and mean velocity:

$$\frac{\bar{T}}{\bar{T}_\delta} = \frac{\bar{T}_w}{\bar{T}_\delta} + \left(\frac{\bar{u}_\delta}{\bar{T}_\delta}\frac{\partial \bar{T}}{\partial \bar{u}}\bigg|_w\right)\left(\frac{\bar{u}}{\bar{u}_\delta}\right) + \left(\frac{\bar{T}_\delta - \bar{T}_w}{\bar{T}_\delta} - \frac{\bar{u}_\delta}{\bar{T}_\delta}\frac{\partial \bar{T}}{\partial \bar{u}}\bigg|_w\right)\left(\frac{\bar{u}}{\bar{u}_\delta}\right)^2, \tag{5.2}$$

whose derivative with respect to $\bar{u}$ gives

$$\frac{\partial \bar{T}}{\partial \bar{u}} = \frac{\partial \bar{T}}{\partial \bar{u}}\bigg|_w - \left(\frac{\bar{T}_w - \bar{T}_\delta}{\bar{u}_\delta^2/2} + \frac{2}{\bar{u}_\delta}\frac{\partial \bar{T}}{\partial \bar{u}}\bigg|_w\right)\bar{u}. \tag{5.3}$$

Combining (5.3) and (4.6) with the assumption $\overline{Pr_e} = 1$, we obtain an analytical expression for r_g:

$$r_g = \frac{\bar{T}_w - \bar{T}_\delta}{\bar{u}_\delta^2/(2C_p)} + \frac{2C_p}{\bar{u}_\delta}\frac{\partial \bar{T}}{\partial \bar{u}}\bigg|_w = \frac{\bar{T}_w - \bar{T}_\delta}{\bar{u}_\delta^2/(2C_p)} - \frac{2Pr}{\bar{u}_\delta}\frac{\bar{q}_{yw}}{\bar{\tau}_w}, \tag{5.4}$$

which is constant across the shear region. This is not surprising because, according to (4.3) and (4.4), $\overline{Pr_e}$ can be rewritten as

$$\overline{Pr_e} = \frac{\overline{(\rho v)'u'}}{\overline{(\rho v)'(T' + \phi')}}\frac{\partial \bar{T}/\partial y}{\partial \bar{u}/\partial y} = 1 - \frac{\bar{u}^2}{2(U_w - r_g\bar{u})}\frac{\partial r_g}{\partial \bar{u}}, \tag{5.5}$$

which shows that the assumption $\overline{Pr_e} = 1$ is equivalent to assuming $r_g = \text{const}$. Equation (5.4) further reveals that r_g consists of two parts: $(\bar{T}_w - \bar{T}_\delta)/(\bar{u}_\delta^2/(2C_p))$ and $(2C_p/\bar{u}_\delta)(\partial \bar{T}/\partial \bar{u})|_w$ (or $-(2Pr/\bar{u}_\delta)(\bar{q}_{yw}/\bar{\tau}_w)$). Similar to the recovery factor r defined for an adiabatic wall, the first part can be understood as a nominal recovery factor for a diabatic wall. The second part denotes the contribution to r_g from the non-zero heat flux at the wall. For an adiabatic wall, r_g naturally reduces to the adiabatic recovery factor r.

By using the definition $\bar{T}_{rg} = \bar{T}_\delta + r_g\bar{u}_\delta^2/(2C_p)$, (5.2) can be rewritten as

$$\frac{\bar{T}}{\bar{T}_\delta} = \frac{\bar{T}_w}{\bar{T}_\delta} + \frac{\bar{T}_{rg} - \bar{T}_w}{\bar{T}_\delta}\frac{\bar{u}}{\bar{u}_\delta} + \frac{\bar{T}_\delta - \bar{T}_{rg}}{\bar{T}_\delta}\left(\frac{\bar{u}}{\bar{u}_\delta}\right)^2, \tag{5.6}$$

which has the same quadratic form as the Crocco–Busemann relation and Walz's equation except that the GRA relation adopts the general recovery factor r_g. For an adiabatic flow, (5.6) reduces to Walz's equation.

Figure 2 compares the Crocco–Busemann relation, Walz's equation and the GRA relation with DNS of CTBLs. Walz's equation shows an improvement over the Crocco–Busemann relation, but deviates visibly from DNS when the wall becomes colder. A maximum discrepancy of $\sim$10 % can be observed at about $\bar{u} = 50\%\,\bar{u}_\delta$ for Walz's equation at $M = 4.5$ and $\Theta = 0$, which is similar to Duan & Martín's (2011) DNS of a supersonic CTBL at $M = 5.0$ and $T_w = T_\delta$ (i.e. $\Theta = 0$). In contrast, the GRA relation displays a good collapse with the DNS across the boundary layer, independent of the wall temperature conditions. Similar collapse of the GRA relation with DNS can be found in CCFs and CPFs, as shown in figure 3, which reveals that the GRA relation applies also to fully developed internal flows.

For adiabatic CTBLs, it is known that the mean total temperature has a small overshoot in the outer portion of the boundary layer due to energy conservation (White 2006), which is not accounted for in Walz's equation. Since Walz's equation is a special case of the GRA, this issue of overshoot and energy conservation is relevant to

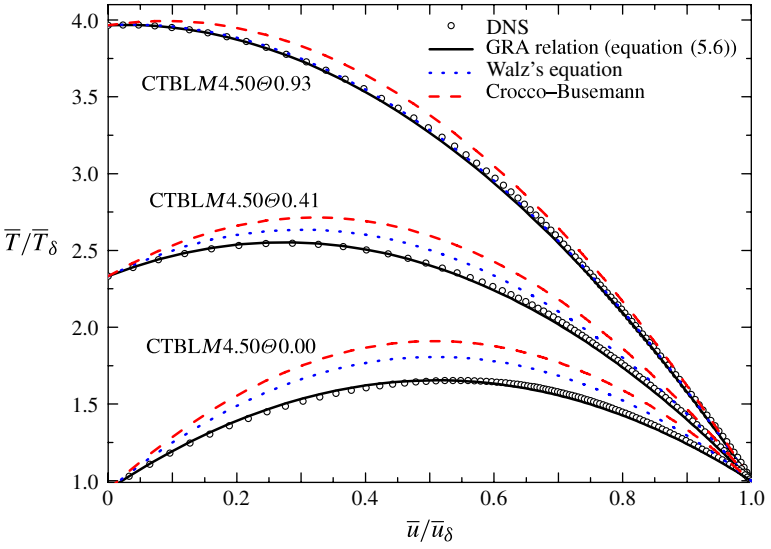

FIGURE 2. (Colour online) Comparison of DNS of CTBLs with the theoretical relationships of Crocco–Busemann, Walz, and the GRA.

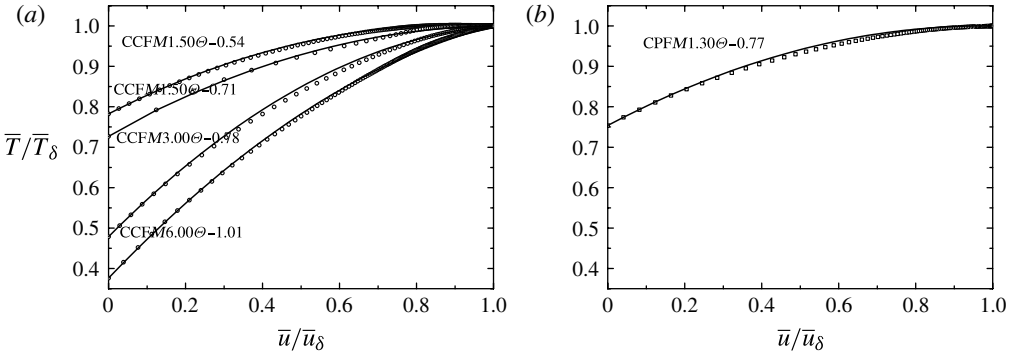

FIGURE 3. Comparison of DNS (symbols, for details see table 1) with the theoretical relationship of GRA (equation (5.6), line) for (*a*) CCFs and (*b*) CPFs; δ denotes channel/pipe centre.

the GRA, which we address now. The open circles in figure 4 show the DNS profile of $\bar{T}_t$ with an overshoot in the outer portion of the boundary layer and a deficiency near the wall. For the adiabatic CTBL at $M = 2.25$, the overshoot of $\bar{T}_t$ is less than 1 % and the deficiency is ∼5.6 % at the wall. The deficiency at the wall will increase to ∼13 % at $M = 4.50$ and 15 % at $M = 6.0$, according to our DNS. The solid line in figure 4 plots $\bar{T}_t$ predicted by the GRA under the adiabatic wall condition (i.e. Walz's equation), showing no overshoot. However, (5.6) describes well the near-wall deficiency, hence can be regarded as a good approximation to the DNS. Similarly in figure 4, the profiles of the relative deviation of $\bar{T}_{ry}$ from its free-stream value are plotted as the open squares for the DNS and the dashed vertical line for the GRA relation (5.6). Again, we find that the GRA relation (5.6) is a good approximation to the DNS, with an error less than 1.5 % across the entire boundary layer. We also

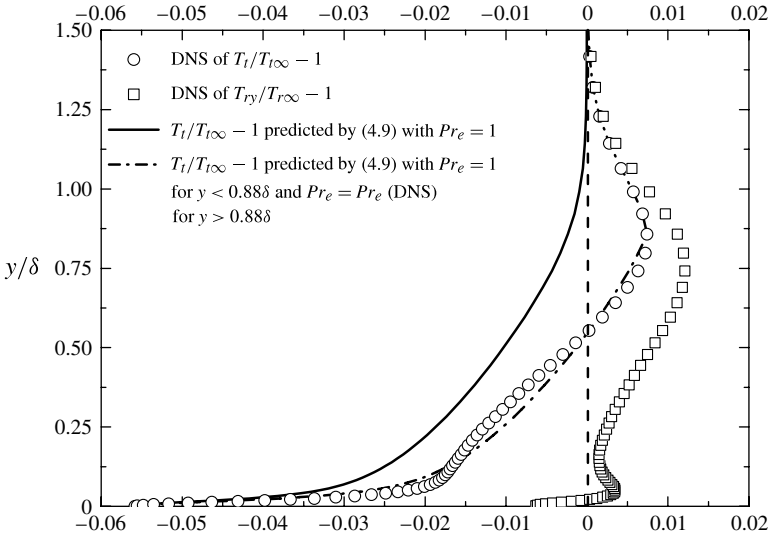

FIGURE 4. Profiles of the relative deviations of $\bar{T}_t$ and $\bar{T}_{ry}$ from their free-stream values for CTBLM2.25Θ0.99 with symbols showing DNS and lines predicted by the GRA relation (4.9).

find that, compared with $\bar{T}_t$, $\bar{T}_{ry}$ is indeed more constant as depicted by (3.23), and importantly, this constancy is independent of Mach number.

On the other hand, one can reproduce the overshoot of $\bar{T}_t$ through integrating the GRA differential equation (4.9) and setting $\overline{Pr}_e = 1$ for $y \leqslant 0.88\delta$ and $\overline{Pr}_e \equiv \overline{Pr}_e(DNS)$ for $y > 0.88\delta$ (the dash-dot line in figure 4). That is to say, the deviation of $\overline{Pr}_e$ from unity in the intermittent layer is systematic, and physically related to the energy conservation in the boundary layer.

To apply (5.6), we need to know both the wall temperature and the ratio of the wall heat flux to the wall shear stress to calculate r_g (see (5.4)). Since the wall temperature and the wall heat flux are interdependent, it is feasible to make a simplification. To do this, we recall the well-known Reynolds analogy factor s defined as

$$s \equiv \frac{2C_h}{C_f} = \frac{\bar{q}_{yw}\bar{u}_\delta}{\bar{\tau}_w C_p(\bar{T}_w - \bar{T}_r)}, \tag{5.7}$$

where $C_f \equiv \bar{\tau}_w/(\bar{\rho}_\delta \bar{u}_\delta^2/2)$ is the skin friction coefficient and $C_h \equiv \bar{q}_{yw}/(\bar{\rho}_\delta \bar{u}_\delta C_p(\bar{T}_w - \bar{T}_r))$ is the heat transfer coefficient, i.e. the Stanton number. Using s, r_g can be rewritten as (see appendix C)

$$r_g = r[sPr + (1 - sPr)\Theta]. \tag{5.8}$$

Note that under the adiabatic wall condition, $\Theta = 1$ and thus $r_g = r$.

Combining (5.6) with (5.8), the GRA relationship for the mean quantities can be rearranged to (see appendix D)

$$\frac{\bar{T}}{\bar{T}_\delta} = \frac{\bar{T}_w}{\bar{T}_\delta} + \frac{\bar{T}_r - \bar{T}_w}{\bar{T}_\delta} f\left(\frac{\bar{u}}{\bar{u}_\delta}\right) + \frac{\bar{T}_\delta - \bar{T}_r}{\bar{T}_\delta}\left(\frac{\bar{u}}{\bar{u}_\delta}\right)^2, \tag{5.9}$$

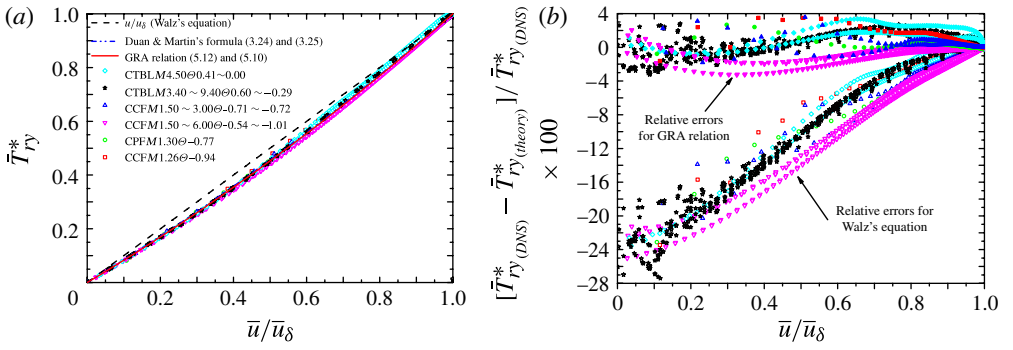

FIGURE 5. (Colour online) (*a*) Profiles of $\bar{T}^*_{ry}$ versus $\bar{u}/\bar{u}_\delta$ (for details of the cases see table 1); (*b*) the relative errors of the GRA relation (equations (5.12) and (5.10)) and Walz's equation.

where

$$f\left(\frac{\bar{u}}{\bar{u}_\delta}\right) = (1 - sPr)\left(\frac{\bar{u}}{\bar{u}_\delta}\right)^2 + sPr\left(\frac{\bar{u}}{\bar{u}_\delta}\right). \tag{5.10}$$

Equations (5.9) and (5.10) are consistent with Duan and Martín's empirical relation (equations (3.25) and (3.24)). Therefore, we give a theoretical derivation of Duan and Martín's formula which identifies their empirical constant α to be

$$\alpha = sPr. \tag{5.11}$$

Equation (5.11) implies that sPr in (5.8) is a constant for at least a number of CWTFs, so that r_g can be estimated by using the wall temperature only.

Using Duan and Martín's definition for $\bar{T}^*_{ry}$, the GRA relation (5.9) can be rewritten as

$$\bar{T}^*_{ry} = f\left(\frac{\bar{u}}{\bar{u}_\delta}\right). \tag{5.12}$$

Figure 5(*a*) displays the collapse of $\bar{T}^*_{ry}$ from our and others' DNS (Huang *et al.* 1995; Ghosh *et al.* 2010; Duan 2011). The DNS include CPF, CCFs, and CTBLs that have Mach numbers covering the range of $M = 1.26 \sim 9.4$, Reynolds numbers of $Re_\tau = 220 \sim 2100$ and diabatic parameters of $\Theta = 0.6 \sim -1.01$. Duan's DNS also consider the effects of high enthalpy and surface catalysis. Therefore, the data collapse in figure 5(*a*) reveals that sPr is approximately a constant for a number of flow cases. It also reveals that the mean relationship of the GRA (equations (5.6) or (5.9)) applies to different $\bar{T}_w$, Re, M, surface catalysis conditions, enthalpy conditions, and flow systems. A simple data fitting shows that $sPr = 0.80 \pm 0.03$, covering Duan and Martín's fitting constant of $\alpha = 0.8259$.

The quality of the data collapse in figure 5(*a*) can further be quantified by plotting the relative deviations between the DNS data and the GRA relation, i.e. $[\bar{T}^*_{ry}(\text{DNS}) - \bar{T}^*_{ry}(\text{theory})]/\bar{T}^*_{ry}(\text{DNS})$. As shown in figure 5(*b*), the deviations are in the range of about $\pm 3.5\,\%$. In comparison, Walz's equation displays a systematic deviation in the shear region. Near the wall, the relative errors of Walz's equation are as large as $-25\,\%$. This systematic deviation is corrected by the GRA relation.

We also deduce from the data collapse in figure 5(*a*) that $s \approx 1.14$ ($sPr \approx 0.80$ when $r = 0.9$) for air flows (Duan *et al.*'s empirical constant $\alpha = 0.8259$ gives $s = 1.18$).

This is consistent with Chi and Spalding's suggestion of $s = 1.16$ ($sPr \approx 0.81$ when $r = 0.89$ as taken in Chi & Spalding (1966)) that applies to diabatic flows at moderate M. In the literature, the Reynolds analogy factor s has been found to vary between 1.0 and 1.2 without a clear trend with $\bar{T}_w$ (or $\bar{q}_{yw}$), Re, M, surface catalysis and enthalpy condition (Bradshaw 1977; Duan 2011). Other factors such as the surface roughness and the turbulence intensity of the incoming flow also affect the value of s (Sons 2005). Not counting the errors due to the difficulties in measuring s, the behaviour of s displays a complexity that needs further studies. However, as revealed by its name, s itself denotes a first level of Reynolds analogy and should be a quantity not very sensitive to the related variables. This constant s leads to great simplicity in applying the mean relationship of the GRA. For the flow case CTBLM4.5Θ0.93, the error in calculating the mean temperature by assuming $sPr = 0.80$ is less than 1.5 % compared with the DNS. In a few exceptions where s varies significantly, e.g. the CTBLs with a pressure gradient, Duan and Martín's empirical constant should be replaced by sPr with s taking the measured value. In this regard, the GRA defines the scope of where Duan and Martín's empirical relation can be applied.

There are a few more points that are worth addressing. Duan & Martín (2011) have observed that the mean temperature–velocity relationship is influenced by both the enthalpy condition and the surface catalysis. Now, under the GRA, this influence acts solely by changing the wall temperature (thus r_g). This can be tested by further studies. In addition, the collapse in figure 5(a) can only be realized by setting $r = 0.9$ for CPFs and CCFs, which reveals that CPFs and CCFs share the same adiabatic recovery factor as that of the adiabatic CTBLs. This is non-trivial because there is no theoretical prediction of this value to our knowledge and it is difficult to measure it through experiments, or DNS that employs a streamwise homogeneity scheme. Finally, we note that the GRA relation (equations (5.12) and (5.10)) suggests a method for measuring the Reynolds analogy factor s through the profiles of mean temperature and mean velocity. The method does not need to measure the skin friction and the wall heat flux, or even the mean profiles of temperature and velocity very near the wall, all of which are challenging to measure.

6. GRA relationships for the fluctuating temperature and the fluctuating velocity

The relationship between the fluctuating temperature T' and the fluctuating velocity u' has been derived and shown by (4.10), where ϕ' should be modelled. A convenient model for ϕ' is $\phi' = (\overline{(\rho v)'\phi'}/\overline{(\rho v)'u'})u'$, so that (4.10) is reduced to

$$T' = \frac{1}{\overline{Pr_t}}\frac{\partial \bar{T}}{\partial \bar{u}}u'. \tag{6.1}$$

Equation (6.1) means that T' and u' are strongly correlated, which, unfortunately, has been invalidated (Guarini *et al.* 2000; Maeder *et al.* 2001; Duan 2011). Therefore, (6.1) is generally not true in the instantaneous fields of CWTFs. However, using DNS data, we can prove that the r.m.s. of T' and u' are approximately related by the coefficient $(1/\overline{Pr_t})(\partial \bar{T}/\partial \bar{u})$ as (6.1) suggests:

$$\sqrt{\overline{T'^2}} = \left|\frac{1}{\overline{Pr_t}}\frac{\partial \bar{T}}{\partial \bar{u}}\right|\sqrt{\overline{u'^2}} = \pm\frac{\overline{(\rho v)'T'}}{\overline{(\rho v)'u'}}\sqrt{\overline{u'^2}}, \tag{6.2}$$

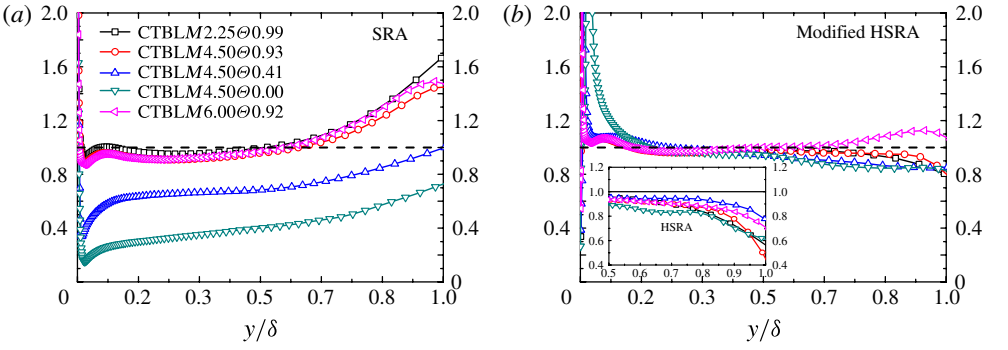

FIGURE 6. (Colour online) Comparisons between the DNS of CTBLs and the theoretical relations of (*a*) SRA, and (*b*) modified HSRA derived by the GRA. HSRA is plotted in the inset.

or equivalently

$$\frac{\sqrt{\overline{T'^2}}/\bar{T}}{(\gamma-1)\,M^2\sqrt{\overline{u'^2}}/\bar{u}} = \frac{1}{|\overline{Pr}_t(\partial\bar{T}_t/\partial\bar{T}-1)|}. \tag{6.3}$$

In (6.2), the plus sign applies to the flow region where the wall-normal gradients of the mean temperature and the mean velocity have the same sign, whereas the minus sign applies to the opposite situation. The different signs are a result of the crucial vortex dynamics in wall-bounded turbulence (Duan, Beekman & Martín 2010). For the CCFs and CPFs, the low-temperature region is generally located near the wall. The ejections of the low-speed/low-temperature fluid and the sweeps of the high-speed/high-temperature fluid result in the same sign for the correlations $\overline{(\rho v)'T'}$ and $\overline{(\rho v)'u'}$ (see (6.2)). The opposite situation happens in, for example, adiabatic CTBLs, where the high-temperature region is located near the wall, so that $\overline{(\rho v)'T'}$ becomes positive whereas $\overline{(\rho v)'u'}$ remains negative.

Equation (6.2) expresses the analogy between the normalized rates of the turbulent heat and momentum transfers as pointed out by Guarini *et al.* (2000). Applying the approximations of $\overline{(\rho v)'T'} \approx \bar{\rho}\overline{v'T'}$ and $\overline{(\rho v)'u'} \approx \bar{\rho}\overline{v'u'}$, (6.3) is equivalent to $R_{v'u'} \approx \pm R_{v'T'}$, which reveals that the turbulence-induced wall-normal transfer of heat closely resembles that of momentum. In other words, the temperature field resembles a passive scalar field, consistent with Morkovin's viewpoint (Morkovin 1962). $R_{v'u'} \approx \pm R_{v'T'}$ has been validated by many studies and is the basis of HSRA (Guarini *et al.* 2000).

Equation (6.3) is equivalent to (6.2) and has the same form as that of HSRA ((1.2) with $a = Pr_t$) except that (6.3) takes a slightly different definition for the turbulent Prandtl number. We call (6.3) a modified HSRA. Figure 6 compares SRA (3.13), HSRA and the modified HSRA with the DNS of CTBLs at different M, Re_τ and Θ. To visualize clearly, figure 6 plots the ratio of the left-hand sides of SRA, HSRA and the modified HSRA to their right-hand sides, following the convention. Figure 6(*b*) shows that the modified HSRA is in good agreement with the DNS across the boundary layer except near the wall. In contrast, SRA is valid below $\sim 0.7\delta$ and only for quasi-adiabatic flows, and an increased and significant deviation from the DNS is observed in CTBLs over cooled walls (figure 6*a*). Such a behaviour for the

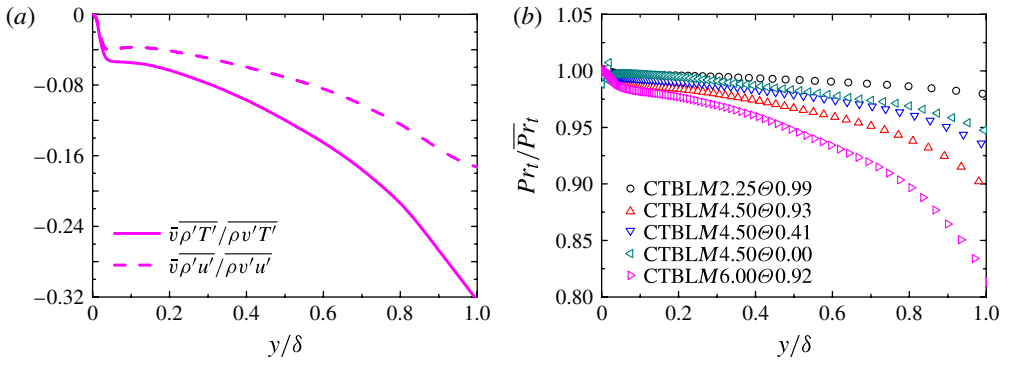

FIGURE 7. (Colour online) The wall-normal profiles of (*a*) $\bar{v}\overline{\rho'T'}/\overline{\rho v'T'}$ and $\bar{v}\overline{\rho'u'}/\overline{\rho v'u'}$ for CTBLM6.00Θ0.92; (*b*) $Pr_t/\overline{Pr}_t$ in CTBLs at different M and Θ.

SRA has been observed in the previous studies (Duan *et al.* 2010; Duan & Martín 2011). HSRA is plotted in the inset of figure 6(*b*). As observed by many researchers (Guarini *et al.* 2000; Duan 2011; Pirozzoli & Bernardini 2011), HSRA agrees with the DNS data much better than the SRA. However, comparison between HSRA and the modified HSRA shows that, in the outer portion of the boundary layers of adiabatic $M = 4.5$ and $M = 6.0$ flows, the modified HSRA exhibits a clear improvement over HSRA. The differences between the modified HSRA and HSRA are ∼10 % and 20 % at the boundary edge for CTBLM4.50Θ0.93 and CTBLM6.00Θ0.92, respectively.

Here we discuss the reason behind the improvement of the modified HSRA. Since $\overline{Pr_t} = Pr_t(1 + \bar{v}\overline{\rho'u'}/\overline{\rho v'u'})/(1 + \bar{v}\overline{\rho'T'}/\overline{\rho v'T'})$, the difference between $\overline{Pr}_t$ and Pr_t lies in the difference between the ratios of $\bar{v}\overline{\rho'T'}/\overline{\rho v'T'}$ and $\bar{v}\overline{\rho'u'}/\overline{\rho v'u'}$, which takes place only in a CTBL. Figure 7(*a*) shows the profiles of $\bar{v}\overline{\rho'T'}/\overline{\rho v'T'}$ and $\bar{v}\overline{\rho'u'}/\overline{\rho v'u'}$ in the DNS case CTBLM6.00Θ0.92. The effect of non-zero $\bar{v}$ and ρ' on the wall-normal heat flux is more than 30 % of $\overline{\rho v'T'}$ at the boundary layer edge, whereas this effect on the Reynolds stress is only 18 % of $\overline{\rho v'u'}$. Such a difference reflects notably on the turbulent Prandtl numbers. Figure 7(*b*) shows that there is a clear difference between Pr_t and $\overline{Pr}_t$ and this difference increases with increasing Mach number and wall-normal coordinate. Hence, the improvement of the modified HSRA over HSRA in the outer portion of the boundary layer is systematic and substantial at high Mach numbers. A reason for this improvement is that, in the validation of the GRA (see § 4.2), we find that the use of $\overline{(\rho v)'X'}$ (instead of $\overline{\rho v'X'}$) captures more quantities which are significant near the edge of the boundary layers. This is because $(\rho v)'$, the wall-normal movement of a fluid mass, is responsible for the turbulent transfer of heat and momentum. More studies are necessary to assess if the improvement of the modified HSRA is meaningful, especially for hypersonic CTBLs.

The success of the SRA for the quasi-adiabatic CTBLs in figure 6(*a*) can be explained by using (6.3), whose right-hand side can be rewritten as

$$\frac{1}{-\overline{Pr}_t(\partial\bar{T}_t/\partial\bar{T} - 1)} = -\frac{1}{\overline{Pr}_t}\frac{C_p}{\bar{u}}\frac{\partial\bar{T}}{\partial\bar{u}} = \frac{1}{\overline{Pr}_t}\left(r_g - \frac{C_p}{\bar{u}}\frac{\partial\bar{T}}{\partial\bar{u}}\bigg|_w\right), \tag{6.4}$$

where the assumption $\overline{Pr}_e = 1$ is applied. For a quasi-adiabatic CTBL, the right-hand side of (6.4) is $r/\overline{Pr}_t$. Since r and $\overline{Pr}_t$ are quantitatively close to each other in measurements and DNS (which may not be accidental), $r/\overline{Pr}_t \approx 1$ and the SRA

works approximately as displayed by the $\Theta \approx 1$ cases in figure 6(*a*). This answers the question of why (3.13) of the SRA is satisfied under the incorrect assumption of negligible total temperature fluctuations, as raised in § 3.1 and by several other researchers (Gaviglio 1987; Guarini *et al.* 2000). For cooled-wall CTBLs, however, the deviation from unity caused by the local modification of $(C_p/\bar{u})(\partial\bar{T}/\partial\bar{u})|_w$ and the global change of r_g becomes more and more significant with the increase of heat flux at the wall, resulting in the failure of the SRA.

One may equally ask the question of why (6.2) and (6.3) are satisfied when (6.1) is not true in the instantaneous fields of general CWTFs. We propose an explanation for this. Equation (4.10) can be rewritten as

$$T' + \phi' = \frac{1+\varepsilon}{\overline{Pr_t}}\frac{\partial\bar{T}}{\partial\bar{u}}u', \tag{6.5}$$

whose mean square is

$$\overline{T'^2} + \overline{\phi'^2} + 2\overline{T'\phi'} = \left(\frac{1}{\overline{Pr_t}}\frac{\partial\bar{T}}{\partial\bar{u}}\right)^2\overline{u'^2} + (2\varepsilon+\varepsilon^2)\left(\frac{1}{\overline{Pr_t}}\frac{\partial\bar{T}}{\partial\bar{u}}\right)^2\overline{u'^2}. \tag{6.6}$$

Then (6.2) is satisfied provided that

$$\overline{\phi'^2} + 2\overline{T'\phi'} = (2\varepsilon+\varepsilon^2)\overline{T'^2} \approx (\overline{Pr_t}^2 - 1)\overline{T'^2}. \tag{6.7}$$

Equation (6.7) can be seen as the reason for the validity of the modified HSRA, or HSRA that has originally been proposed in a phenomenological way (Gaviglio 1987). The reason underlying (6.7) is not clear to us at present.

In quasi-adiabatic flows, $\phi' \approx -T'_{rg}$, so (6.7) becomes

$$\frac{\overline{T'^2_{rg}} - 2\overline{T'T'_{rg}}}{\overline{T'^2}} \approx \overline{Pr_t}^2 - 1. \tag{6.8}$$

Guarini *et al.* (2000) pointed out that the success of the SRA equation (3.13) for adiabatic flows was a consequence of $(\overline{T_t'^2} - 2\overline{T'T_t'})/\overline{T'^2} = 0$, instead of $\overline{T_t'^2} = 0$. We are able to clarify that this also is a rough approximation by comparing with (6.8). Figure 8 shows that $\overline{T'^2_{rg}} - 2\overline{T'T'_{rg}}$ is smaller than $\overline{T'^2}$ but not negligible ($\sim 20\,\%\overline{T'^2}$), and it is correctly approximated by $(\overline{Pr_t}^2 - 1)\overline{T'^2}$ in most of the shear region. In contrast, $\overline{T_t'^2} - 2\overline{T'T_t'} = 0$ is only roughly satisfied ($\sim 15\,\%\overline{T'^2}$), similar to Guarini *et al.*'s (2000) plot of an adiabatic CTBL at $M = 2.5$.

The correlation coefficient $R_{u'T'}$ is another topic in the Reynolds analogy theories. A linear relationship between T' and u', such as that of the SRA and (6.1), inevitably results in a unity $|R_{u'T'}|$ that disagrees with experiments and DNS (Gaviglio 1987; Smith & Smits 1993; Guarini *et al.* 2000; Maeder *et al.* 2001; Pirozzoli *et al.* 2004; Duan 2011). By using the GRA, the behaviour of $R_{u'T'}$ with respect to the wall-normal coordinate and the wall temperature condition can be understood more clearly. Combination of (6.5) and the assumption $\overline{Pr_e} = 1$ yields

$$T' + \phi' = \frac{\partial\bar{T}}{\partial\bar{u}}u'. \tag{6.9}$$

In adiabatic flows, T' and ϕ' (i.e. $-T'_{rg}$) are quantitatively comparable but ϕ' is not necessarily strongly correlated with u' (due to (4.4)), so T' and u' cannot be strongly correlated. In the literature, $|R_{u'T'}|$ in quasi-adiabatic flows is found to

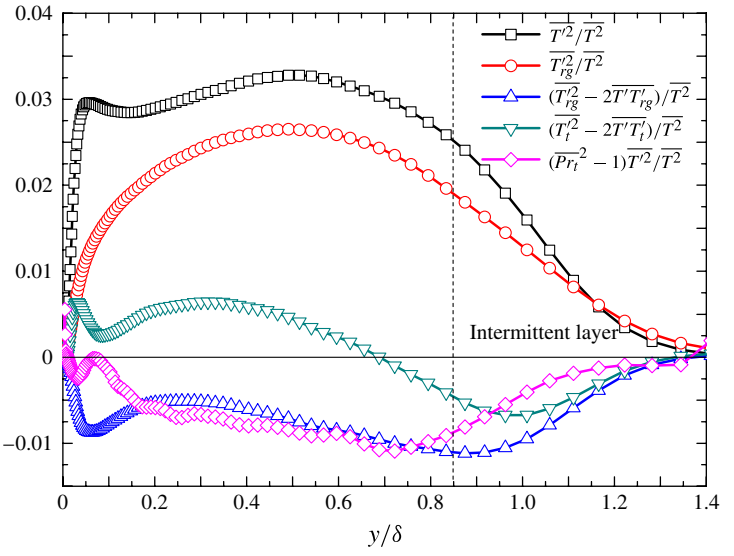

FIGURE 8. (Colour online) Comparison of the terms: $\overline{T'^2}/\overline{T}^2$; $\overline{T'^2_{rg}}/\overline{T}^2$; $(\overline{T'^2_{rg}} - 2\overline{T'T'_{rg}})/\overline{T}^2$; $(\overline{T'^2_t} - 2\overline{T'T'_t})/\overline{T}^2$ and $(\overline{Pr_t}^2 - 1)\overline{T'^2}/\overline{T}^2$. The DNS data are for CTBLM4.5Θ0.93.

be approximately $0.6 \sim 0.9$, significantly deviating from unity (Guarini *et al.* 2000; Maeder *et al.* 2001; Pirozzoli *et al.* 2004; Duan *et al.* 2011). In diabatic flows, $R_{u'T'}$ is affected by the sign and the modulus of $\partial\bar{T}/\partial\bar{u}$: $R_{u'T'}$ and $\partial\bar{T}/\partial\bar{u}$ share the same sign and the discrepancy between $|R_{u'T'}|$ and unity is inversely related to the magnitude of $\partial\bar{T}/\partial\bar{u}$ (see (6.9)). Therefore, we could deduce that, in the outer portion of a cooled CTBL, $R_{u'T'}$ is quasi-constant and increases from -1 with decreasing Θ (figure 9). The latter is because $\partial\bar{T}/\partial\bar{u} = (\partial\bar{T}/\partial\bar{u})|_w - (r_g\bar{u}/C_p)$ (see (5.3)): the magnitude of $|\partial\bar{T}/\partial\bar{u}|$ becomes smaller as a result of the larger positive $(\partial\bar{T}/\partial\bar{u})|_w$ and the smaller positive r_g. The quite constant distribution of $R_{u'T'}$ is because $\bar{u}$ varies only a little in the outer portion of the boundary layer. In the near-wall region of a cooled CTBL, $\bar{T}$ would reach maximum near the location where $R_{u'T'}$ has a sign transition (Duan *et al.* 2010), and most variation of $R_{u'T'}$ happens there (figure 9). We could make similar a deduction for the profiles of $R_{u'T'}$ in heated CTBLs, or in CCFs and CPFs under arbitrary wall temperature conditions. Figure 9 confirms our argument which suggests that a linear relationship between T' and u', such as (6.1), is only possibly closely satisfied in the shear regions of CTBLs on over-heated or CPFs/CCFs on over-cooled walls. For a flow having an extreme in the $\bar{T}$ profile, such as cooled CTBLs in the near-wall region, one has $\sqrt{\overline{\phi'^2}} = \sqrt{\overline{T'^2}}$ near the extremal point according to (6.5). Consequently, (6.2) would not be satisfied. This explains why (6.3) significantly deviates from the DNS in the near-wall region of the cooled wall CTBLs (figure 6*b*).

7. Discussion

7.1. *The approximations and assumptions in the GRA*

In the derivation of the GRA, we have adopted several approximations that limit the application of the GRA. The chief approximation is that of quasi-one-dimensional flow. It is well accepted in canonical wall-bounded turbulent flows, but it also sets a strong

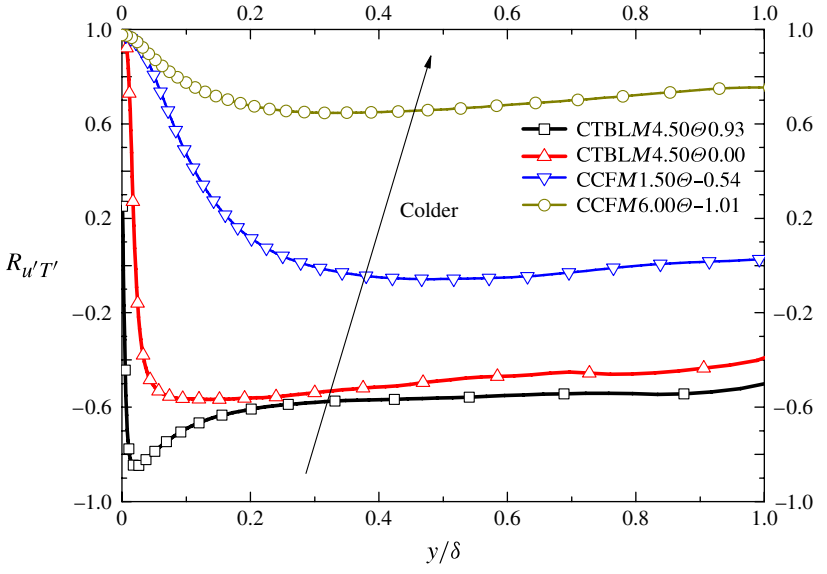

FIGURE 9. (Colour online) Variation of the correlation coefficient $R_{u'T'}$ with the diabatic parameter Θ for CTBLs and CCFs.

requirement that prohibits an incautious application of the GRA in CWTFs that have separation or transversal flow, very strong acceleration/deceleration, large temperature gradient along the wall, very rough surface, intense interactions with an impinging shock, or a protruding object, or a flow that impinges on or leaves the wall, etc.

We have made a key assumption that $\overline{Pr_e} = 1$ in the shear region of a CWTF, independent of Pr, wall temperature, streamwise pressure gradient, etc. This assumption leads to a uniform profile for the general recovery factor, and a quadratic formula between the mean temperature and the mean velocity that applies quite well to different flow systems under general diabatic wall conditions. However, as is shown, $\overline{Pr_e} = 1$ is only approximate in real turbulence (figure 1*a*) and cannot describe the overshoot of the mean total temperature near the edge of an adiabatic CTBL (figure 4). More studies are necessary to assess if $\overline{Pr_e} = 1$ is still valid at other Re (especially low Re) and M (especially high M), strong pressure gradient, Pr significantly smaller than unity (where the turbulent Prandtl number may be much larger than unity, see Kays 1994), and with large surface roughness, wall blowing and suction, free-stream turbulence, etc.

To derive the GRA relationship for the fluctuation fields, a convenient model for the residual temperature ϕ' has been introduced. Since no non-trivial relation could exist for the instantaneous fluctuations, we turn to seeking the reason for the validity of the modified HSRA. Equation (6.7) is identified to be this relation satisfied by the fluctuation fields which relates the residue temperature ϕ' and the static temperature fluctuation T' with the turbulent Prandtl number $\overline{Pr_t}$. For quasi-adiabatic flows, (6.7) improves the argument of Guarini *et al.* (2000) to explain the success of the SRA (i.e. (3.13)). Although (6.7) can be validated by the current DNS, the mechanism behind it remains unknown.

To simplify the application of the GRA, we have also employed the observation of Duan & Martín (2011) to assume that sPr is almost constant for a large number

of CWTFs. Although it greatly simplifies the application of the GRA with a good accuracy, more studies should be conducted, especially on the Reynolds analogy factor s whose behaviour remains unclear (Sons 2005).

Perhaps the most important assumption in the GRA is as that of the SRA: (4.3) and (4.4) are solutions to the Reynolds-averaged momentum and energy equations, which can be written in a similar form for general CWTFs. Guarini *et al.* (2000) preferred not to identify them as solutions, but the assumption (4.4) implies the relation (4.3). Then a question arises: Why does the GRA hold universally in the CWTFs? The GRA relationships for the fluctuating temperature and velocity reveal that the temperature field closely resembles a passive scalar field, consistent with Morkovin's hypothesis (Morkovin 1962). Therefore, the universality of the GRA actually reflects the common turbulence mechanisms in wall-bounded turbulent flows. Specifically, the essential dynamics of the large-scale coherent structures in the bulk of wall-bounded turbulent flows are similar, without being significantly influenced by compressibility, wall temperature condition, pressure gradient, or flow situation far away from the wall (which differentiates CCF/CPF from CTBL) (Morkovin 1962; Duan 2011). Since the turbulent transport of momentum and heat is dominated similarly by vortical structures, universal analogy solutions for the velocity and temperature fields are reasonable, first the instantaneous analogy of (4.4) due to the turbulent eddies, and then the mean-field analogy of (4.3). We could thus speculate that, when the acoustic component of the fluctuating motion plays an important role, such as in highly compressible mixing layers and possibly in CTBLs at very high Mach numbers, the basis of the GRA might not hold. This requires further investigations.

7.2. *Several key parameters emerging in the GRA*

One of GRA's successes stems from the introduction of the general recovery factor r_g. As revealed by (5.8), r_g includes the effects of the Prandtl number, wall temperature, the adiabatic recovery factor, and the Reynolds recovery factor that encompasses more complex effects such as those of pressure gradient and surface roughness (Sons 2005). Therefore, r_g is a significant generalization of the adiabatic recovery factor r. A uniform profile for r_g is an adequate approximation since it gives a rather simple relation between the mean temperature and the mean velocity, with a minimal modification to the Crocco–Busemann relation and Walz's equation but at a higher accuracy and applied to a wider range of flows. For a specific flow, r_g is approximately uniquely determined by the diabatic parameter Θ, which makes the application of the GRA very simple: only the wall temperature is involved.

The diabatic parameter Θ in (5.8) is a dimensionless parameter for characterizing the wall temperature effects in diabatic CWTFs. In these flows, three control parameters are generally involved: M, Re, and a dimensionless wall temperature that, we argue, has not been well defined up to now. To study the M-effect, one has to compare flows with different M at the same Re and the same dimensionless wall temperature, whose definitions are not trivial owing to the nonlinear coupling between the different physical mechanisms they represent. Some studies have used T_w/T_δ or T_w/T_f (where T_f is a reference temperature) to define the dimensionless wall temperature (Duan *et al.* 2010). Note that Θ in (5.8) is the unique parameter to determine r_g, and hence the mean temperature–velocity relationship in flows under different wall temperature conditions. Therefore, Θ is a well-founded dimensionless parameter that can be applied to study, for example, the M-effects of diabatic compressible wall-bounded turbulence. This requires further study.

The effective turbulent Prandtl number $\overline{Pr_e}$ is another key parameter emerging in the GRA. As shown by (4.9), it is $\overline{Pr_e}$ that determines the relationship between the mean temperature and the mean velocity. $\overline{Pr_e}$ is a modification to the turbulent Prandtl number $\overline{Pr_t}$: the effect of the residual temperature ϕ' is included additionally. Since $\bar{\phi}'$ is zero, $\overline{(\rho v)'\phi'}$ represents a background energy flux that is non-negligible in CWTFs. As revealed by the assumption $\overline{Pr_e} = 1$, this background results in a systematic deviation of Pr_t from unity, important information for turbulence models ending up with the idea of eddy viscosity and eddy heat conductivity (Dong & Zhou 2010). The assumption $\overline{Pr_e} = 1$, as has been discussed, needs further study to reveal its mechanism and envelope in the parameter space.

8. Conclusions

Here we have proposed a generalized Reynolds analogy for compressible wall-bounded turbulent flows, and validated the theory by DNS of CTBLs, CCFs and CPFs over diabatic walls. The GRA is obtained by a formal generalization of the SRA, in which we introduce a general recovery factor that accounts for the effects of Pr, wall temperature, pressure gradient, etc. Also, we discard the 'strong' Reynolds analogy assumption by introducing the residual temperature ϕ', which remedies the fatal flaw of the SRA. By doing this, we are able to prove that the GRA that consists of (4.3), (4.4) and (4.6) is a solution to the Reynolds-averaged momentum and energy equations for CWTFs.

The GRA leads to new relationships between temperature and velocity. We clarify that it is the effective Prandtl number $\overline{Pr_e}$ that connects the mean temperature and the mean velocity. This $\overline{Pr_e}$ is very close to unity across the shear region and insensitive to the flow conditions. By assuming $\overline{Pr_e} = 1$, we derive the mean relationship of the GRA, which is a close approximation to the real turbulence and has a similar quadratic form to the Crocco–Busemann relation and Walz's equation except that the general recovery factor r_g is applied. Factor r_g is found to be constant in the shear region under the assumption $\overline{Pr_e} = 1$. We reveal that r_g depends on the adiabatic recovery factor, Prandtl number, Reynolds analogy factor, and the diabatic parameter that is introduced by us and shown to be a key dimensionless temperature. Thus we are able to derive Duan and Martín's empirical relation that applies to a number of flow conditions (M, Re, wall temperature, enthalpy condition, surface catalysis, etc.). We further elucidate that Duan and Martín's empirical constant is actually the product of Prandtl number and the Reynolds analogy factor, which suggests a method for measuring the Reynolds analogy factor by using the mean profiles of temperature and velocity. By using DNS of CTBLs, CCFs and CPFs under different wall temperature conditions, we validate the mean temperature–velocity relationship of the GRA. The GRA relation agrees with the DNS very well. In comparison, Walz's equation shows a 10 % over-estimation of the mean temperature in cooled CTBLs.

We derive from the GRA the HSRA that has been proposed phenomenologically and validated by numerous studies. The reason for the validity of HSRA is identified. A slight modification to HSRA is also shown to improve it. Using the GRA, the variation of the correlation coefficient $R_{u'T'}$ with respect to wall temperature and wall-normal coordinate is explained. The deviation of the turbulent Prandtl number from unity is shown to be systematic and related to the residual temperature ϕ'.

The GRA proposed herein unveils a systematic similarity in the complex nonlinear coupling between the thermal and velocity fields of general CWTFs, and paves the way to predicting the mean fields of compressible wall-bounded turbulence with

information on the corresponding incompressible flow. Also, as discussed, many issues left unresolved about the GRA require further investigations.

Acknowledgements

The authors thank the referees for their constructive comments, which clearly improved the quality of the manuscript. Also the authors want to express many thanks to Y. Z. Wang, S. Ghosh and S. Pirozzoli for sharing their DNS data, to J. Chen, X. Chen, Y. Z. Wang, X. L. Li, X. Liang, D. X. Fu, and P. Martin for helpful discussions, to SSC (Shanghai) and NSCC (Tianjin) for providing computational resources. This work is supported by NSFC under Grants No. 11621062, No. 10921202 and No. 50806002, and MOST 973 Project under Grant No. 2009CB724100.

Appendix A

Expanding (3.2) and (3.3) with (3.1) gives

$$\overline{\rho u}\partial_x\tilde{u} + \overline{\rho v}\partial_y\tilde{u} = -\partial_x\bar{p} + \partial_y[(\overline{\tau_{xy}} - \overline{(\rho v)'u'})] + \partial_x[\overline{\tau_{xx}} - \overline{(\rho u)'u'}], \tag{A 1}$$

$$\begin{aligned}\overline{\rho u}\partial_x\tilde{H} + \overline{\rho v}\partial_y\tilde{H} = {}& \partial_x(\overline{u\tau_{xx}}) + \partial_x(\overline{v\tau_{xy}}) + \partial_y(\overline{u\tau_{xy}}) + \partial_y(\overline{v\tau_{yy}}) \\ & - \partial_x\overline{(\rho u)'H'} - \partial_y\overline{(\rho v)'H'} - \partial_x(\bar{q}_x) - \partial_y(\bar{q}_y).\end{aligned} \tag{A 2}$$

Neglecting the small terms including $\partial_y(\overline{v\tau_{yy}})$, $\partial_x(\overline{\tau_{xx}})$, $\partial_x(\overline{u\tau_{xx}})$, $\partial_x(\overline{v\tau_{xy}})$, $\partial_x\overline{(\rho u)'u'}$, $\partial_x\overline{(\rho u)'H'}$ and $\partial_x(\bar{q}_x)$, (A 1) and (A 2) can be simplified with the aid of the approximations $\overline{uf} \approx \bar{u}\bar{f}$ and (3.4) to give (4.11) and (4.12), respectively.

Appendix B

First, we give the following relations:

$$\tilde{H} = \bar{H}_g + (1 - r_g)\tilde{u}^2/2, \tag{B 1}$$

$$\bar{u}\bar{\mu}\partial_y\bar{u} = \bar{\mu}\partial_y(\bar{H}_g) - \bar{\mu}\partial_y\bar{h} + \bar{\mu}\partial_y[(1 - r_g)\tilde{u}^2/2], \tag{B 2}$$

$$\overline{(\rho v)'H'} = \overline{(\rho v)'H'_g} + (1 - r_g)\bar{u}\overline{(\rho v)'u'}, \tag{B 3}$$

$$\overline{(\rho v)'h'} = (U_w - r_g\bar{u})\overline{(\rho v)'u'} - C_p\overline{(\rho v)'\phi'}, \tag{B 4}$$

$$(\bar{\mu}\tilde{u}^2/2)\partial_y(r_g) = (U_w - r_g\bar{u})[\bar{\tau} + \overline{(\rho v)'u'}] + Pr\bar{q}_y. \tag{B 5}$$

The total stress $\bar{\tau}$ in (B 5) is defined as $\bar{\tau} \equiv \bar{\mu}\partial_y\bar{u} - \overline{(\rho v)'u'}$. Equations (B 1)–(B 3) come from definition, (B 4) comes from (4.4) and (B 5) is a result of multiplying the derivative (with respect to y) of (4.3) by $\bar{\mu}$. The substitution of (B 1)–(B 3) into (4.12) gives (4.14), in which

$$\begin{aligned}f(r_g) = {}& \overline{\rho u}\partial_x[(r_g - 1)\tilde{u}^2/2] + \overline{\rho v}\partial_y[(r_g - 1)\tilde{u}^2/2] \\ & - \partial_y[(r_g - 1)\bar{u}\bar{\tau} + (\bar{\mu}\tilde{u}^2/2)\partial_y(r_g) + (1 - Pr)\bar{q}_y].\end{aligned} \tag{B 6}$$

Multiplying the momentum equation (4.11) by $U_w - \bar{u}$, one has

$$\overline{\rho u}\partial_x[U_w\bar{u} - \tilde{u}^2/2] + \overline{\rho v}\partial_y[U_w\bar{u} - \tilde{u}^2/2] = -(U_w - \bar{u})\partial_x\bar{p} + (U_w - \bar{u})\partial_y\bar{\tau}. \tag{B 7}$$

Replacing $U_w\bar{u}$ with $\bar{H}_g - \bar{H}_w$ (see (4.3)) in the left-hand side of (B 7) yields

$$\begin{aligned}& \overline{\rho u}\partial_x\bar{h} + \overline{\rho v}\partial_y\bar{h} + \overline{\rho u}\partial_x[(r_g - 1)\tilde{u}^2/2] + \overline{\rho v}\partial_y[(r_g - 1)\tilde{u}^2/2] \\ & \quad = -(U_w - \bar{u})\partial_x\bar{p} + (U_w - \bar{u})\partial_y\bar{\tau}.\end{aligned} \tag{B 8}$$

Subtracting $\bar{u}$ times (4.11) from (4.12), a further arrangement of (B 4) gives

$$\overline{\rho u}\partial_x\bar{h} + \overline{\rho v}\partial_y\bar{h} = -\partial_y[(U_w - r_g\bar{u})\overline{(\rho v)'u'} - C_p\overline{(\rho v)'\phi'} + \overline{q_y}] + \bar{u}\partial_x\bar{p} + \bar{\tau}\partial_y\bar{u}. \quad \text{(B 9)}$$

Substituting (B 9) into (B 8) gives

$$\begin{aligned}\overline{\rho u}\partial_x[(r_g-1)\bar{u}^2/2] + \overline{\rho v}\partial_y[(r_g-1)\bar{u}^2/2] = \partial_y[(U_w - r_g\bar{u})\overline{(\rho v)'u'} - C_p\overline{(\rho v)'\phi'} + \overline{q_y}] \\ - (U_w - \bar{u})\partial_x\bar{p} + U_w\partial_y\bar{\tau} - \partial_y(\bar{u}\bar{\tau}) - \bar{u}\partial_x\bar{p}.\end{aligned} \quad \text{(B 10)}$$

Substituting (B 10) and (B 5) into (B 6), a calculation yields $f(r_g) = -U_w\partial_x\bar{p} - C_p\partial_y\overline{(\rho v)'\phi'}$, the constraint required to guarantee the similarity between the momentum and energy equations in § 4.2.

Appendix C

With (5.4), r_g can be further written as

$$\begin{aligned} r_g &= \frac{\bar{T}_r - \bar{T}_\delta}{\bar{u}_\delta^2/(2C_p)}\left(\frac{\bar{T}_w - \bar{T}_\delta}{\bar{T}_r - \bar{T}_\delta} + \frac{\bar{u}_\delta}{\bar{T}_r - \bar{T}_\delta}\left.\frac{\partial\bar{T}}{\partial\bar{u}}\right|_w\right) \\ &= r\left(\frac{\bar{T}_w - \bar{T}_\delta}{\bar{T}_r - \bar{T}_\delta} + \frac{\bar{T}_r - \bar{T}_w}{\bar{T}_r - \bar{T}_\delta}\frac{\bar{u}_\delta}{\bar{T}_r - \bar{T}_w}\left.\frac{\partial\bar{T}}{\partial\bar{u}}\right|_w\right). \end{aligned} \quad \text{(C 1)}$$

Because $(\bar{u}_\delta/(\bar{T}_r - \bar{T}_w))(\partial\bar{T}/\partial\bar{u})|_w = sPr$, $(\bar{T}_r - \bar{T}_w)/(\bar{T}_r - \bar{T}_\delta) = 1 - ((\bar{T}_w - \bar{T}_\delta)/(\bar{T}_r - \bar{T}_\delta))$ and $(\bar{T}_w - \bar{T}_\delta)/(\bar{T}_r - \bar{T}_\delta) = \Theta$, one has

$$r_g = r[\Theta + (1-\Theta)sPr] = r[sPr + (1 - sPr)\Theta]. \quad \text{(C 2)}$$

Appendix D

According to the definitions of $\bar{T}_{rg}$ and $\bar{T}_r$, one has

$$\begin{aligned}\bar{T}_{rg} &= \bar{T}_r + (r_g/r - 1)(r\bar{u}_\delta^2/(2C_p)) \\ &= \bar{T}_r + (sPr - 1)(1-\Theta)(\bar{T}_r - \bar{T}_\delta) = \bar{T}_r + (sPr - 1)(\bar{T}_r - \bar{T}_w).\end{aligned} \quad \text{(D 1)}$$

Substituting (D 1) into (5.6), one has

$$\begin{aligned}\frac{\bar{T}}{\bar{T}_\delta} = \frac{\bar{T}_w}{\bar{T}_\delta} + \frac{\bar{T}_r - \bar{T}_w + (sPr-1)(\bar{T}_r - \bar{T}_w)}{\bar{T}_\delta}\frac{\bar{u}}{\bar{u}_\delta} \\ + \frac{\bar{T}_\delta - \bar{T}_r - (sPr-1)(\bar{T}_r - \bar{T}_w)}{\bar{T}_\delta}\left(\frac{\bar{u}}{\bar{u}_\delta}\right)^2.\end{aligned} \quad \text{(D 2)}$$

Rearranging (D 2) gives

$$\frac{\bar{T}}{\bar{T}_\delta} = \frac{\bar{T}_w}{\bar{T}_\delta} + \frac{\bar{T}_r - \bar{T}_w}{\bar{T}_\delta}\left[(1-sPr)\left(\frac{\bar{u}}{\bar{u}_\delta}\right)^2 + sPr\frac{\bar{u}}{\bar{u}_\delta}\right] + \frac{\bar{T}_\delta - \bar{T}_r}{\bar{T}_\delta}\left(\frac{\bar{u}}{\bar{u}_\delta}\right)^2, \quad \text{(D 3)}$$

which is (5.9).

REFERENCES

BRADSHAW, P. 1977 Compressible turbulent shear layers. *Annu. Rev. Fluid Mech.* **9**, 33–52.

BRUN, C., PETROVAN BOIARCIUC, M., HABERKORN, M. & COMTE, P. 2008 Large eddy simulation of compressible channel flow. *Theor. Comput. Fluid Dyn.* **22** (3), 189–212.

BUSEMANN, A. 1931 *Handbuch der Experimentalphysik, vol. 4*. Geest und Portig.

CEBECI, T. & SMITH, A. M. O. 1974 *Analysis of Turbulent Boundary Layers*. Academic.

CHI, S. W. & SPALDING, D. B. 1966 Influence of temperature ratio on heat transfer to a flat plate through a turbulent boundary layer in air. In *International Heat Transfer Conference, 3 RD, Chicago, Illinois*, pp. 41–49.

CROCCO, L. 1932 Sulla trasmissione del calore da una lamina piana a un fluido scorrente ad alta velocita. *L Aerotecnica* **12**, 181–197.

DEBIÈVE, J. F. 1976 Contribution à l'étude du comportement d'un écoulement compressible turbulent ($M = 2.3$) soumis à des gradients élevés de vitesse et de pression. *Doctorat de spécialité Univ. d'Aix Marseille II*.

DEBIEVE, J.-F, GOUIN, H. & GAVIGLIO, J. 1982 Momentum and temperature fluxes in a shock wave-turbulence interaction. *Struct. Turbul. Heat Mass Transfer* **1**, 277–296.

DONG, M. & ZHOU, H. 2010 The improvement of turbulence modelling for the aerothermal computation of hypersonic turbulent boundary layers. *Sci. China* G: *Phys. Mech. Astron.* **53** (2), 369–379.

DUAN, L. 2011 DNS of hypersonic turbulent boundary layers. PhD thesis, Princeton University.

DUAN, L., BEEKMAN, I. & MARTÍN, M. P. 2010 Direct numerical simulation of hypersonic turbulent boundary layers. Part 2. Effect of wall temperature. *J. Fluid Mech.* **655**, 419–445.

DUAN, L., BEEKMAN, I. & MARTÍN, M. P. 2011 Direct numerical simulation of hypersonic turbulent boundary layers. Part 3. Effect of Mach number. *J. Fluid Mech.* **672**, 245–267.

DUAN, L. & MARTÍN, M. P. 2011 Direct numerical simulation of hypersonic turbulent boundary layers. Part 4. Effect of high enthalpy. *J. Fluid Mech.* **684**, 25–59.

GATSKI, T. B. & BONNET, J. P. 2009 *Compressibility, Turbulence and High Speed Flow*. Elsevier.

GAVIGLIO, J. 1987 Reynolds analogies and experimental study of heat transfer in the supersonic boundary layer. *Intl J. Heat Mass Transfer* **30** (5), 911–926.

GHOSH, S., FOYSI, H. & FRIEDRICH, R. 2010 Compressible turbulent channel and pipe flow: similarities and differences. *J. Fluid Mech.* **648**, 155–181.

GUARINI, S. E., MOSER, R. D., SHARIFF, K. & WRAY, A. 2000 Direct numerical simulation of a supersonic turbulent boundary layer at Mach 2.5. *J. Fluid Mech.* **414**, 1–33.

HOPKINS, E. J. & INOUYE, M. 1971 An evaluation of theories for predicting turbulent skin friction and heat transfer on flat plates at supersonic and hypersonic Mach numbers. *AIAA J.* **9** (6), 993–1003.

HOWARTH, L. 1953 *Modern Developments in Fluid Dynamics: High Speed Flow, vol.1*. Clarendon.

HUANG, P. G., COLEMAN, G. N. & BRADSHAW, P. 1995 Compressible turbulent channel flows: DNS results and modelling. *J. Fluid Mech.* **305**, 185–218.

JIANG, L.-Y. & CAMPBELL, I. 2008 Reynolds analogy in combustor modelling. *Intl J. Heat Mass Transfer* **51** (5), 1251–1263.

KAYS, W. M. 1994 Turbulent Prandtl number – where are we? *J. Heat Transfer* **116**, 284–295.

LADERMAN, A. J. 1978 Effect of wall temperature on a supersonic turbulent boundary layer. *AIAA J.* **16** (7), 723–729.

LADERMAN, A. J. & DEMETRIADES, A. 1974 Mean and fluctuating flow measurements in the hypersonic boundary layer over a cooled wall. *J. Fluid Mech.* **63**, 121–144.

LI, X.-L., FU, D.-X. & MA, Y.-W. 2006 Direct numerical simulation of a spatially evolving supersonic turbulent boundary layer at $Ma = 6$. *Chin. Phys. Lett.* **23** (6), 1519–1522.

LI, X., MA, Y. & FU, D. 2001 DNS and scaling law analysis of compressible turbulent channel flow. *Sci. China* A: *Maths* **44** (5), 645–654.

MAEDER, T., ADAMS, N. A. & KLEISER, L. 2001 Direct simulation of turbulent supersonic boundary layers by an extended temporal approach. *J. Fluid Mech.* **429**, 187–216.

MORKOVIN, M. V. 1962 Effects of compressibility on turbulent flows. In *Mecanique de la Turbulence* (ed. A. Favre), pp. 367–380. CNRS.

OWEN, F. K., HORSTMAN, C. C. & KUSSOY, M. I. 1975 Mean and fluctuating flow measurements of a fully-developed, non-adiabatic, hypersonic boundary layer. *J. Fluid Mech.* **70** (2), 393–413.

PIROZZOLI, S. & BERNARDINI, M. 2011 Turbulence in supersonic boundary layers at moderate Reynolds number. *J. Fluid Mech.* **688**, 120–168.

PIROZZOLI, S., GRASSO, F. & GATSKI, T. B. 2004 Direct numerical simulation and analysis of a spatially evolving supersonic turbulent boundary layer at *M*. *Phys. Fluids* **16** (3), 530–545.

REYNOLDS, O. 1874 On the extent and action of the heating surface of steam boilers. *Manchester Lit. Phil. Soc.* ***14****, 7–12 (reproduced in Reynolds, O. 1961 On the extent and action of the heating surface of steam boilers. Intl J. Heat Mass Transfer* ***3*** *(2), 163–166).*.

RUBESIN, M. W. 1990 Extra compressibility terms for favre-averaged two-equation models of inhomogeneous turbulent flows. *NASA STI/Recon Tech. Rep.* N 90, 23701.

SHE, Z.-S., CHEN, X., WU, Y. & HUSSAIN, F. 2010 New perspective in statistical modelling of wall-bounded turbulence. *Acta Mechanica Sin.* 1–15.

SHE, Z. S., WU, Y., CHEN, X. & HUSSAIN, F. 2012 A multi-state description of roughness effects in turbulent pipe flow. *New J. Phys.* **14** (9), 093054.

SHESHAGIR, K. & PARANJPE, P. A. 1969 Skin friction in compressible turbulent boundary layers. *AIAA J.* **7** (4), 793–796.

SMITH, D. R. & SMITS, A. J. 1993 Simultaneous measurement of velocity and temperature fluctuations in the boundary layer of a supersonic flow. *Exp. Therm. Fluid Sci.* **7** (3), 221–229.

SMITS, A. J. & DUSSAUGE, J. P. 2006 *Turbulent Shear Layers in Supersonic Flow*. Springer.

SONS, J. 2005 A critical assessment of Reynolds analogy for turbine flows. *J. Heat Transfer* **127** (5), 472–485.

SPALDING, D. B. & CHI, S. W. 1964 The drag of a compressible turbulent boundary layer on a smooth flat plate with and without heat transfer. *J. Fluid Mech.* **18**, 117–143.

SPINA, E. F., SMITS, A. J. & ROBINSON, S. K. 1994 The physics of supersonic turbulent boundary layers. *Annu. Rev. Fluid Mech.* **26** (1), 287–319.

STALKER, R. J. 2005 Control of hypersonic turbulent skin friction by boundary-layer combustion of hydrogen. *J. Spacecr. Rockets* **42** (4), 577–587.

VAN DRIEST, E. R. 1951 Turbulent boundary layer in compressible fluids. *J. Aeronaut. Sci.* **18** (3), 145–160; (Also available in 'Van Driest, E. R. 2003 Turbulent boundary layer in compressible fluids. *J. Spacecr. Rockets* **40** (6), 1012–1028').

WALZ, A. 1962 *Compressible Turbulent Boundary Layers*, pp. 299–350 CNRS.

WALZ, A. 1966 *Strömungs-und Temperaturgrenzschichten*. Braun (translation in *Boundary Layers of Flow and Temperature*, MIT Press, 1969).

WANG, Y.-Z. 2012 A multi-layer theory for mean field prediction in compressible channel flow (in Chinese). PhD thesis, Peking University.

WHITE, F. M. 2006 *Viscous Fluid Flow*. McGraw-Hill.

WHITFIELD, D. L. & HIGH, M. D. 1977 Velocity-temperature relations in turbulent boundary layers with nonunity Prandtl numbers. *AIAA J.* **15** (3), 431–434.

ZHANG, Y.-S., BI, W.-T., HUSSAIN, F., LI, X.-L. & SHE, Z.-S. 2012 Mach-number-invariant mean-velocity profile of compressible turbulent boundary layers. *Phys. Rev. Lett.* **109** (5), 054502.